Universidade de Lisboa

Faculdade de Farmácia

3-hydroxy-V-coumarin hydrolysis study through fluorometry and LC-MS analysis

Margarida Sofia Bento Ferreira

Trabalho de campo orientado pelo Professor Seppo Auriola, University of Eastern Finland e coorientado pela Professora Doutora Noélia Duarte, Professora Auxiliar da Faculdade de Farmácia da Universidade de Lisboa.

Mestrado Integrado em Ciências Farmacêuticas

2023

Universidade de Lisboa

Faculdade de Farmácia

3-hydroxy-V-coumarin hydrolysis study through fluorometry and LC-MS analysis

Margarida Sofia Bento Ferreira

Trabalho Final de Mestrado Integrado em Ciências Farmacêuticas apresentado à Universidade de Lisboa através da Faculdade de Farmácia

Trabalho de campo orientado pelo Professor Seppo Auriola, University of Eastern Finland e coorientado pela Professora Doutora Noélia Duarte, Professora Auxiliar da Faculdade de Farmácia da Universidade de Lisboa.

2023

Resumo

As cumarinas são uma classe de lactonas presentes na natureza, com uma estrutura resultante da fusão de um anel benzénico com uma α-pirona. Estes compostos exibem uma ampla variedade de propriedades terapêuticas, tendo despertado o interesse da indústria farmacêutica nos últimos anos. A sua estrutura e caraterísticas físico-químicas possibilitam a formação de inúmeros derivados sintéticos que funcionam como *scaffolds* privilegiados, capazes de atingir objetivos terapêuticos específicos em diversas doenças. As cumarinas π-expandidas revelam características espectrofotométricas específicas, tais como maior deslocamento de Stokes e atributos colorimétricos. Estas características atraíram os investigadores, o que levou ao desenvolvimento da 3-hidroxi-V-cumarina, cujo metabolismo e potencial terapêutico nunca foram estudados. A identificação e caracterização de metabolitos nas fases iniciais do desenvolvimento de fármacos é crucial para avaliar os seus efeitos farmacológicos e toxicológicos, o que auxilia na exclusão precoce de candidatos tóxicos ou não efetivos. Por isso, este trabalho de investigação teve como propósito o estudo da hidrólise da 3-hidroxi-V-cumarina e dos seus metabolitos.

Para verificar a variação da quantidade da 3-hidroxi-V-cumarina na presença de citosol foi utilizado o método espectrofluorimétrico, uma vez que este composto apresenta fluorescência. A cromatografia líquida acoplada à espectrometria de massa, foi a técnica analítica eleita para corroborar os resultados obtidos por fluorimetria e para detetar e identificar os metabolitos resultantes da hidrólise da 3-hidroxi-V-cumarina, uma vez que apresenta elevada sensibilidade e seletividade. Foi também investigada a influência de parâmetros físicos nomeadamente o pH na hidrólise da 3-hidroxi-V-cumarina. Este projeto incluiu o estudo da cinética desta reação de hidrólise com a determinação dos parâmetros cinéticos na presença de citosol hepático humano, bem como a comparação das atividades enzimáticas entre diferentes espécies.

Este projeto compreendeu a fase inicial do estudo do metabolismo da 3-hidroxi-V-cumarina, com foco na reação de hidrólise que se previa ocorrer tendo em conta a estrutura química do composto. Estudos posteriores de metabolismo serão conduzidos, nomeadamente estudos das reações de fase II, de forma a complementar a informação obtida neste trabalho.

Palavras-chave: 3-hidroxi-V-cumarina, Hidrólise, Fluorometria, Cromatografia líquida, Espectrometria de massa.

Abstract

Coumarins are a naturally occurring class of lactones with a fused benzene ring and α-pyrone structure. These compounds display a wide variety of therapeutic properties, which has sparked interest in the pharmaceutical industry in recent years. Its structure and physicochemical characteristics enable the formation of numerous synthetic derivatives that function as privileged scaffolds, capable of targeting specific therapeutic objectives in several diseases. Chromeno[3,4-c]chromene-6,7-diones are π-expanded coumarins that reveal specific spectrophotometric characteristics, such as larger Stokes shift and colorimetric attributes. These characteristics attracted researchers and led to the development of 3-hydroxy-V-coumarin, whose metabolism and therapeutic potential have never been studied. Identifying and characterizing metabolites in the initial drug development phases is crucial to evaluating their pharmacological and toxicological effects. This helps in the early exclusion of candidates that may be toxic or ineffective. Thus, this research work studied the hydrolysis of 3-hydroxy-V-coumarin and its metabolites.

To assess the variation in the quantity of 3-hydroxy-V-coumarin in the presence of cytosol, the spectrofluorimetric method was employed, as this compound exhibits fluorescence. Liquid chromatography coupled with mass spectrometry was the analytical method chosen to corroborate the findings from fluorometry and to detect and identify the metabolites resulting from the hydrolysis of 3-hydroxy-V-coumarin, as it presents high sensitivity and selectivity. The influence of physical parameters on the hydrolysis of 3-hydroxy-V-coumarin, specifically pH, was also investigated. Additionally, this project included a study of the hydrolysis reaction kinetics with the determination of kinetic parameters in the presence of human liver cytosol, as well as a comparison of enzymatic activity among different species.

This project comprised the initial phase of investigating the metabolism of 3-hydroxy-V-coumarin, with a focus on the hydrolysis reaction expected based on the chemical structure of this compound. Subsequently, further metabolism studies will be conducted, including the examination of phase II reactions to complement the information obtained through this project.

Keywords: 3-hydroxy-V-coumarin, Hydrolysis, Fluorometry, Liquid Chromatography, Mass spectrometry.

Acknowledgments

I want to start by thanking my mother and father for always being my greatest source of support and courage. They always believed in me and helped me get to where I am. A special acknowledgment goes to my sister Madalena for being my best friend, most of the time, and for always supporting and challenging me. My gratitude extends to my grandparents who constantly express the pride they have in me, and who celebrate all my achievements. I must also extend my thanks to Diogo for always being a huge support, and always wanting the best for me. Without them, I certainly wouldn't have succeeded.

I would also like to thank all my friends, especially those who were true companions at the Faculty of Pharmacy of the University of Lisbon: Maria, Joana, Francisca, Teresa, and Sara. We've shared a lot of moments in the past years, and without a doubt, nothing would have been the same without them.

I express my greatest gratitude to Professor Seppo Auriola who played a very important role in my integration in Finland and greatly supported this project, and to Professor Risto Juvonen for all his help, care, constant availability, and for his desire to show the best of Finland. I also would like to thank Professor Noélia Duarte for her help and availability in recent months.

Finally, I want to express my greatest thanks to Finland and especially to Kuopio, for giving me the best experience of my life, for the wonderful friendships, and for once again showing me that the best things happen when we leave our comfort zone. This place will forever have a huge place in my heart.

Abbreviations

AChE	Acetylcholinesterase
ADME	Absorption, distribution, metabolism, and excretion
BChE	Butyrylcholinesterase
BSA	Bovine serum albumin
CE	Capillary electrophoresis
DMAP	Dimethylaminopyridine
ESI	Electrospray ionization
FTMS	Fourier transform mass spectrometry
GC	Gas chromatography
HPLC	High-performance liquid chromatography
HRMS	High-resolution mass spectrometry
ICT	Intramolecular charge transfer
LC	Liquid chromatography
LRMS	Low-resolution mass spectrometry
MAO	Monoamine oxidase
MS	Mass spectrometry
MS/MS	Tandem mass spectrometry
NMR	Nuclear magnetic resonance spectroscopy
PD	Pharmacodynamic
PK	Pharmacokinetics
PON	Paraoxonase
RP	Reversed-phase
RT	Retention time
TOF	Time-of-flight
UHPLC	Ultra high-performance liquid chromatography

Table of contents:

List of Figures

List of Tables

1. Introduction

Every day in the chemical and pharmaceutical industry, researchers evaluate new molecules with possible therapeutic potential, often synthetic derivatives of compounds present in nature, as with synthetic coumarin derivatives. However, it is not enough to evaluate the therapeutic potential of these molecules, it is necessary to evaluate their fate in the body because this could be a factor that leads to the exclusion of the use of these molecules. To carry out this assessment, there are numerous analytical methods and equipment, and those that present the most suitable characteristics for the analysis of each compound must be used (1–3).

1.1 Pharmacokinetics

Pharmacokinetics (PK) attends to the study of absorption, distribution, metabolism, and excretion (ADME) of drugs in the body, essentially exploring how the body interacts with the drug. However, it also integrates the evaluation of associated toxicity (4). ADME is of great importance in the drug design field as it helps in identifying scaffolds of interest through a simplified approach. For drugs to produce their intended pharmacological effects after administration, they must reach the designated site(s) of action in the body. Nonetheless, if drugs exhibit inadequate pharmacokinetic characteristics like high clearance, short half-life (t1/2), and low bioavailability after oral administration, their pharmacodynamic effects (PD) will remain below ideal results (5).

1.2. Drug metabolism

Implementing an optimal process for drug discovery and development continues to be one of the most significant challenges for the pharmaceutical research community. The field of drug metabolism holds a significant position in the discovery and development of drugs, as it strongly contributes to understanding the pharmacological and toxicological effects of a drug in humans (5). As drugs can undergo substantial biotransformation that modifies their intended effects, metabolism studies are now conducted during the initial phases of the drug development process. This allows the removal of numerous potentially unsafe or ineffective candidates in the initial phases (2). Research in the drug metabolism field plays an important role in enhancing lead compounds to achieve optimal PK/PD attributes, uncovering new chemical entities by identifying active metabolites, and mitigating potential safety concerns resulting from the formation of reactive or harmful metabolites (5). The study of drug metabolism thus

serves two purposes: first, to discover the role and destiny of the drug, and second, to manipulate the metabolic pathway of a potential medication (6).

The metabolism of drugs in the body is a complex biotransformation process, where drugs undergo structural modifications resulting in the formation of several molecules (metabolites) through the action of different metabolizing enzymes. The main aim of this process is to act as an inherent detoxification mechanism in the human body, offering a way to protect against environmental hostility, which includes endogenous and exogenous molecules (5). Generally, drug metabolism leads to the formation of a compound that is more water-soluble, facilitating its efficient excretion by the liver, kidneys, and/or gastrointestinal tract (7). Drug metabolism is categorized into phase I reactions, which involve processes like oxidation, reduction, and hydrolysis, and phase II reactions, which include conjugation reactions like glucuronidation and sulfation. Frequently, drugs undergo initial metabolism by phase I enzymes (mainly CYP450s), which mediate the exposure or introduction of a functional group (such as −OH, −NH2, −SH, or −COOH), followed by subsequent conjugation by phase II enzymes responsible for adding an endogenous conjugate to the polar group added in phase I (6,8,9). Typically, these reactions lead to metabolites with reduced biological activity. However, there are situations when reactive and potentially more toxic metabolites are generated (6). The metabolism of drugs in humans is subject to variability and can be influenced by numerous internal and external factors. Age, gender, pregnancy, various disease conditions, solid organ transplantation, medication usage, and genetic polymorphism can impact this process (7).

The liver is the main site in the body for metabolizing drugs and external toxins, as well as internal compounds (7,10). Conducting in vitro metabolism investigations using human and animal tissue preparations, such as the liver (fresh or cryopreserved hepatocytes and hepatic subcellular components), or in vivo metabolism studies involving animals are valuable strategies to identify the principal metabolic pathways of drugs (5,10,11).

1.3. Hydrolysis

Hydrolysis is a chemical reaction in which a substance is decomposed into its constituent units through the addition of water. Hydrolysis can occur through chemical and enzymatic processes and constitutes one of the most important mechanisms for the metabolism of xenobiotics in mammals (12).

Mammals have several enzymes that can hydrolyze xenobiotics with functional groups such as carboxylic acid esters, amides, thioesters, carbamates, phosphoric acid esters, acid anhydrides, lactones, and thiolactones. The main enzymes responsible for hydrolysis are carboxylesterases, cholinesterases, and paraoxonases (lactonases) (12).

1.3.1. Hydrolysis of lactones

In the case of drugs containing lactones, hydrolysis easily takes place through enzymatic and non-enzymatic mechanisms. This hydrolysis process strongly impacts the bioavailability and effectiveness of drugs and prodrugs containing lactones (2,13). Figure 1 illustrates the hydrolysis reaction of a lactone.

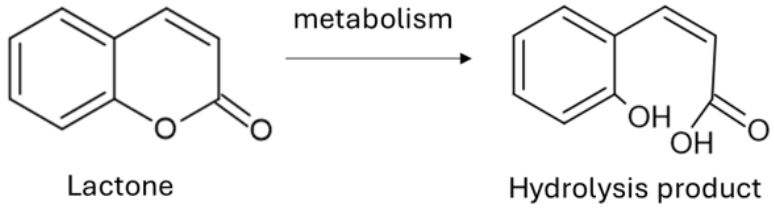

Figure 1. Hydrolysis of a lactone.

Numerous techniques are available to monitor the presence of a lactone and its hydrolysis products, assuming that a standard for each compound is available and no other alterations are taking place beyond lactone hydrolysis. A few examples include fluorometry, high-performance liquid chromatography (HPLC) coupled with ultraviolet or fluorescence detection, and mass spectrometry (MS). The identification of lactone hydrolysis in unknown compounds, particularly when other modifications occur, is possible through mass spectrometry. Given that this technique provides low detection limits and allows rapid data acquisition and analysis, detecting lactone hydrolysis is achievable by utilizing distinctive fragmentation patterns in MS/MS data. This characterization method is relevant for metabolites of lactone-containing pharmaceuticals that have been previously identified but lack structural characterization (2).

1.3.2. Paraoxonases

Paraoxonases are calcium-dependent enzymes located on human chromosome 7 that catalyze the hydrolysis of a diverse range of compounds including organophosphates, organophosphinites, esters of aromatic carboxylic acids, cyclic carbonates, lactones, and

oxidized phospholipids. These enzymes contain a critical sulfhydryl group (-SH), making them susceptible to inhibition by EDTA, metal ions, and various mercury-based compounds (8,14).

Humans express three paraoxonases known as PON1, PON2, and PON3. PON1 can be found in liver microsomes and plasma, where it is linked solely with high-density lipoprotein (HDL). PON2 is not present in plasma, but it is expressed in the inner mitochondrial membrane of vascular cells and many other tissues. PON3 is expressed in liver and kidney microsomes and plasma. All three PONs have a high level of specificity in relation to their substrates, with overlapping, but distinct substrates (8,14). Only PON1 has significant arylesterase activity and the capability to hydrolyze paraoxon, which is the active metabolite of the organophosphate insecticide parathion (15). Despite being closely related to PON1, PON2 and PON3 exhibit almost no true "paraoxonase" activity (14). Despite this, all three enzymes have the capability to hydrolyze a range of lactones, considered the main physiological role of PONs, besides their other catalytic activities (12).

PONs exhibit a much faster rate of hydrolysis for lactones compared to their respective non-cyclic ester analogs. All three PONs specifically hydrolyze lipophilic lactone rings with five and six members (i.e., γ- and δ-lactones). This suggests that these compounds serve as good representations of the natural substrates for PONs. The active site of PON3 appears to be larger than that of PON2 and PON1, which gives it a greater capacity to hold and hydrolyze bulky substrates. On the other hand, PON1 has a stronger ability to catalyze the hydrolysis of non-substituted and short-chain-substituted lactones. The lactonase activity of PON2, however, is much more restricted. The biological activity of lactones can impact cellular growth, signaling, and differentiation. As a result, it is likely that PONs play a crucial role in health and diseases by metabolizing lactones and altering their biological activity, both endogenous and exogenous (8,14).

1.4. Coumarin and its derivatives

Coumarin (1,2-benzopyrone or 2H-1-benzopyran-2-one) and its derivatives are a type of polyphenolic compounds categorized in a group of colorless and crystalline oxygenated heterocyclic compounds (16). Their distinctive structure is composed of interconnected pyrone and benzene rings, with the pyrone carbonyl group at position 2, as illustrated in Figure 2. Coumarins are commonly present in nature, with coumarin itself being initially isolated from

tonka bean (*Dipteryx odorata*), and numerous additional coumarin derivatives being identified across a broad family of plants (3,17).

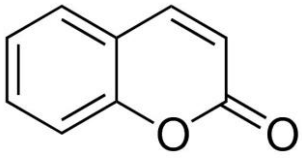

Figure 2. Chemical structure of Coumarin.

Coumarins exhibit great versatility, having applications in the areas of biology, medicine, perfumery, and cosmetics. In recent years, coumarins aroused interest due to their elevated fluorescence quantum yield, large Stokes shift, exceptional light stability, and reduced toxicity (18). Their conjugated double-ring system provides multiple opportunities for chemical modifications, facilitating the generation of a wide range of derivatives that are highly appealing and versatile to medicinal and biological chemists. Special emphasis is given to the potential of coumarins as a significant scaffold in drug design, along with their utility as fluorescent probes for prodrug decaging, metal detection, and diagnostic purposes. Coumarins have been identified with anticarcinogenic, antimicrobial, antioxidant, anti-inflammatory, antihypertensive, anticonvulsant, anticoagulant, and triglycerides lowering properties as well as enzymatic inhibitory activity against α-glucosidase, carbonic anhydrase, tyrosinase, sulfatase, and xanthine oxidase (3,16,19). Moreover, they show promise as anti-neurodegenerative agents through their activity as MAO and AChE/BChE inhibitors. Additionally, hydroxycoumarins have been documented to have a robust antioxidative and protective impact against oxidative stress, as they scavenge reactive oxygen species (3). Studies have shown that substitution patterns can have a positive effect on the therapeutic, pharmacological, and biochemical attributes of coumarins. It is important to clarify the role of coumarins as potential agents that target specific therapeutic goals across various diseases. This comprehension is vital for utilizing coumarins and their substituents as potential prodrugs and incorporating them into complementary therapeutic strategies. Consequently, the investigation of innovative synthetic coumarin derivatives gains importance, given their potential efficacy in addressing diseases (3,19).

1.4.1. π-expanded coumarins

Because of the extension of the conjugated system and the abundance of electrons in coumarin-fused heterocycles, coumarins with an π-expanded system have several notable characteristics.

These include a larger Stokes shift and colorimetric attributes in comparison to traditional coumarins, which typically absorb and emit radiation in a lower wavelength. Considering these significant benefits, π-expanded coumarins can find applications in environmental detection and even biosensors (20,21). By exploring new π-expanded coumarins, researchers synthesized a distinctive family of bis-coumarins that are fused at the pyranone rings, known as chromeno[3,4-c]chromene-6,7-diones, depicted in Figure 3. This cluster of V-shaped bis-coumarins exhibits intense fluorescence within the range of 400−550 nm (22).

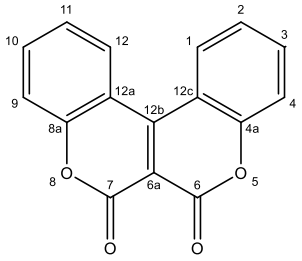

Figure 3. Chemical structure of chromeno[3,4-c]chromene-6,7-dione.

The existence of a hydroxyl group at position 3 in chromeno[3,4-c]chromene-6,7-dione gave rise to 3-hydroxy-V-coumarin, whose metabolism has never been studied before (22). 3-hydroxy-V-coumarin chemical structure and properties are described in Figure 4.

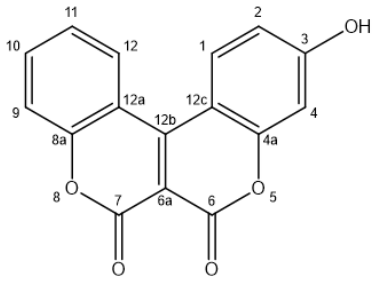

Chemical Formula: $C_{16}H_8O_5$
Exact Mass: 280,03717
Molecular Weight: 280,24
m/z: 280.04 (100.0%), 281.04 (17.3%), 282.04 (1.4%), 282.04 (1.0%)
Elemental Analysis: C, 68.58; H, 2.88; O, 28.55

Figure 4. Chemical structure, chemical formula, exact mass, molecular weight, and elemental analysis of 3-hydroxy-V-coumarin.

The synthesis of this compound involves the reaction of an electron-rich phenol with an ester of coumarin-3-carboxylic acids, leading to the formation of a substituted chromeno[3,4-

c]chromene-6,7-dione, as shown in Figure 5. This reaction is aided by Lewis acids and 4-dimethylaminopyridine (DMAP). The most probable mechanistic pathway includes transesterification catalyzed by either Lewis acids or DMAP, followed by the intramolecular conjugate addition of α,β-unsaturated esters to phenols and the subsequent oxidation of the initially formed intermediate (22).

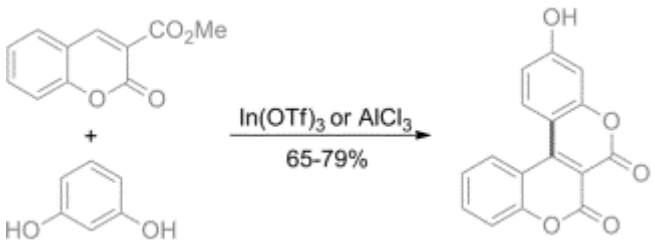

Figure 5. Chemical synthesis of 3-hydroxy-V-coumarin (22).

This V-shaped bis-coumarin presents an electron-donating group (hydroxyl) and an electron-withdrawing group (carbonyl), creating a push-pull electron structure that emits fluorescence in accordance with the Intramolecular Charge Transfer (ICT) theory (20).

1.5. Fluorometry

Fluorescence is a phenomenon in which a molecule, containing fluorophore groups in its structure, absorbs light with consequent emission of light with low energy and at higher wavelengths (23). Fluorophores typically integrate conjugated aromatic groups or cyclic molecules with multiple π bonds or nonbonding electrons. The most important parameters of this process include the absorption maxima (λmax) during excitation and the extinction coefficient at λmax (ε) during emission. Energy loss occurs during excitation due to rapid relaxation to the first singlet excited state (S1) and the reorganization of solvent molecules around the modified dipole of the excited state. Fluorescence occurs when this excited state relaxes to the ground state (S0) by emitting a photon. Each fluorophore exhibits a specific pair of excitation (λmax) and emission maximum (λem) wavelengths (23,24).

In fluorescence spectroscopy (fluorometry) the amount of light emitted after absorption is measured to provide information about the components present in the samples, for example, whether there is decay of a substrate. Fluorescence techniques are extensively used to evaluate the rates and kinetic mechanisms of enzyme reactions, being highly sensitive and specific. This

characteristic becomes particularly important when conducted on limited tissue samples or other sources with minimal enzyme activity (23,24).

As mentioned in 1.4.1., coumarins exhibit a significant π-π conjugated system with electron-rich and charge-transfer properties. The desirable photophysical properties of coumarin and its derivatives make them widely used as fluorophores. This conjugated structure makes them suitable for use as fluorescent sensors in biological activities (23).

1.6. Liquid chromatography - Mass spectrometry

Liquid chromatography in combination with mass spectrometry (LC-MS) is an analytical technique that combines the resolving power of LC with the detection specificity and sensitivity of MS. This technique can be used to provide information about the molecular weight, structure, identity, and quantity of different compounds present in samples with different matrices (25).

LC-MS plays a very important role in the development of new drugs and can be applied to a wide variety of biological molecules at different stages of their development including drug discovery, product characterization, metabolism studies, and identification of impurities and degradation products (25,26). The selectivity, low sample volume requirement, sensitivity, and speed of this technique support its use in the discovery and development of new drugs (27). LC-MS has been increasingly used in xenobiotic metabolism studies to analyze samples derived from in vitro incubations and/or in vivo studies since this method allows rapid identification and partial structural characterization of metabolites with great sensitivity for most drugs of interest and respective metabolites. Factors supporting the increasing use of LC-MS in xenobiotic metabolism studies include high throughput, soft ionization, and good coverage of metabolites (26,28,29). Furthermore, LC-MS facilitates the identification and quantification of metabolites by reducing sample complexity and allowing separation before detection (30).

1.6.1. Liquid chromatography

Effective chromatographic performance is necessary to have sufficient specificity for LC-MS analysis (31). Chromatographic separation can reduce the complexity of samples and minimize matrix interaction effects when ionization is performed in mass spectrometry, improving MS detection sensitivity and data quality by reducing background noise (28). Considering the above, high-performance separation techniques are required and liquid chromatography is the most popular option in metabolism studies (32).

Until 2010, the separation method that dominated metabolism studies was High-performance liquid chromatography (HPLC), however, in recent years, Ultra-high-performance liquid chromatography (UHPLC), a more powerful version of LC, has become the preferred technique (32). UHPLC is the gold standard for LC-MS analysis in drug metabolism studies, as it is associated with higher throughput, sensitivity, and selectivity than HPLC (27). Furthermore, this method offers an excellent separation with short analysis times due to high efficiency (32).

Reversed-phase (RP) LC is the most used in the analysis of metabolites due to the universality of the method and the fact that it is compatible with the most used MS ionization sources (31). The RP mode consists of a nonpolar stationary phase and a polar mobile phase. The stationary phase is made up of saturated aliphatic groups chemically linked to silanol sites of silica particles, with octadecyl silica (C18) being the most popular RP option. The mobile phase is made up of a polar solvent such as water or methanol. RP-UHPLC thus allows rapid separation of components based on their affinity for each of these phases (32).

1.6.2. Mass Spectrometry

Mass spectrometry allows the identification, characterization, and quantification of analyte molecules based on their molecular masses and fragmentation patterns. This technique is based on three main processes: ion generation (in the ion source); transport and selection of ions in space (high vacuum) according to their mass-to-charge values (*m/z*) (in the mass analyzer); and ion detection (33).

Mass spectrometers operate according to the conversion of the analyte molecules to an ionized state with subsequent analysis of the ions and their fragments that are produced during the ionization process (25).

1.6.2.1. Ionization

The design and type of ionization source of the mass spectrometer are important in the performance of the method. Electrospray ionization (ESI) is the most applied ionization source for biological molecules. It is used when the compounds to be analyzed are thermally labile, nonvolatile, and polar (26). This ionization source facilitates the robust coupling with liquid chromatography, and it is compatible with reversed-phase LC making LC-MS the most obvious choice for quantitative and qualitative analysis in drug metabolism studies (27). ESI uses a high

electricity field to produce charged droplets from a solution leading to the formation of ions in the gas phase (34). Electrospray ionization is a soft source of ionization which means that minimal energy is supplied to the analyte molecule and therefore little fragmentation occurs (25). Furthermore, it does not require derivatization and can ionize compounds of a wide range of masses (34).

The ionization process corresponds to the acquisition of a positive or negative charge to the molecule to be analyzed. In the positive ionization mode, the positive charge is transferred to the molecule by adding a proton ($[M+H]^+$) or forming an adduct with a positively charged molecule present in the solvent (e.g., $[M+NH4]^+$, $[M+Na]^+$). In the negative ionization mode, the analyte molecule can lose a proton ($[M-H]^-$) or the negative charge can be transferred by forming an adduct with an anion (e.g., $[M+formate]^-$, $[M+acetate]^-$). The ion beam generated by ESI is continuously transferred to the high vacuum region through a series of small apertures and focus voltages (25,26,33).

1.6.2.2. Mass analyzers

There are different types of mass analyzers which can be generally summarized as quadrupole, magnetic sector, ion trap, time-of-flight (TOF), or Fourier transform (FT) analyzers, dependent on the physics of mass analysis. They can be further combined to allow the analysis of various analytes and their fragments (MS/MS), or the same analyzer can perform MS and MS/MS (MS^2), and sometimes, an elevated MS^n level (35). Mass analyzers have varying resolution capabilities, with high-resolution instruments (HRMS) such as TOF and FT analyzers capable of providing accurate mass measurements, while low-resolution instruments (LRMS), mainly quadrupole analyzers, have limited resolution, meaning they cannot accurately distinguish ions when their *m/z* ratios are proximate (26,28).

Orbitrap is a member of the Fourier Transform Mass Spectrometry (FTMS) family and represents the first high-performance mass analyzer that employs ion capture in electrostatic fields. The Orbitrap mass analyzer combines high speed with excellent quantification properties (35,36). The high resolution, mass accuracy, and sensitivity of this robust analyzer are essential to meet the demands in numerous areas of research (36,37).

The Orbitrap mass analyzer consists of two symmetrical external cup-shaped electrodes facing each other and electrically isolated, and an internal spindle-shaped electrode that holds the trap and aligns it through dielectric end-spacers. The voltage is applied between the external and

internal electrodes resulting in a linear electric field along the axis and therefore the oscillations are harmonic. Simultaneously, the radial component of the field attracts ions. There is an external injection compartment that works as an ion trap, named C-trap. This compartment allows the storage of a significantly large population of ions for subsequent injection into the Orbitrap analyzer in a short pulse, causing each mass-to-charge (*m/z*) population to form a sub-microsecond pulse. Ions are injected between the external electrodes and the internal electrode, and the radial electric field bends the trajectory of the ions towards the central electrode while the tangential velocity generates an opposing centrifugal force. This causes the ions to maintain a spiral in the trap in ultrahigh vacuum. At the same time, the axial electric field, due to the shape of the electrodes, pulls the ions toward the widest part of the trap, giving rise to harmonic axial oscillations. These oscillations generate image currents that are detected by the external electrodes functioning as collector plates. The image current in the time domain is Fourier transformed to the frequency domain and then converted into a mass spectrum (35,36,38,39). Figure 6 schematizes the Orbitrap mass analyzer constituents.

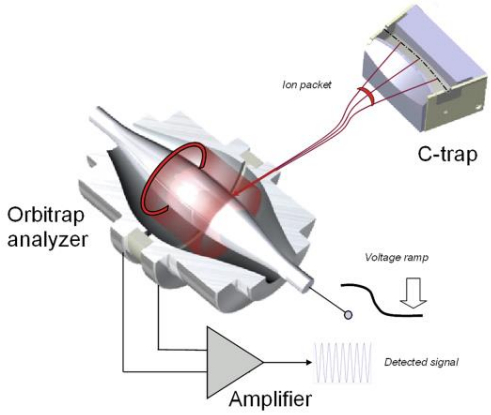

Figure 6. Orbitrap mass analyzer constituents (35).

1.6.3. Tandem mass spectrometry (MS/MS)

In addition to resolving ions based on their mass-to-charge values and obtaining estimates of their molecular masses, mass analyzers can also generate highly resolved and accurate MS/MS spectra to increase the throughput of metabolite identification. Tandem mass spectrometry (MS/MS) offers greater detection specificity in complex matrices than unit-resolution full-scan MS. This is possible due to ionic fragmentation by collision-induced dissociation where specific ions are selected and fragmented. The MS/MS characterization of the metabolites is based on the comparison of the product ion spectra of the metabolites with that of the parent drug and through detailed interpretation of the fragmentation patterns (28,31,40,41).

2. Aims

The main aim of this project is to investigate the hydrolysis metabolism of 3-hydroxy-V-coumarin.

It is intended to identify the hydrolysis products of 3-hydroxy-V-coumarin through LC-MS analysis: if there are one or two different lactone hydrolysis products, and if a product is formed as a result of two consecutive hydrolyses of the two lactones as illustrated in Figure 7.

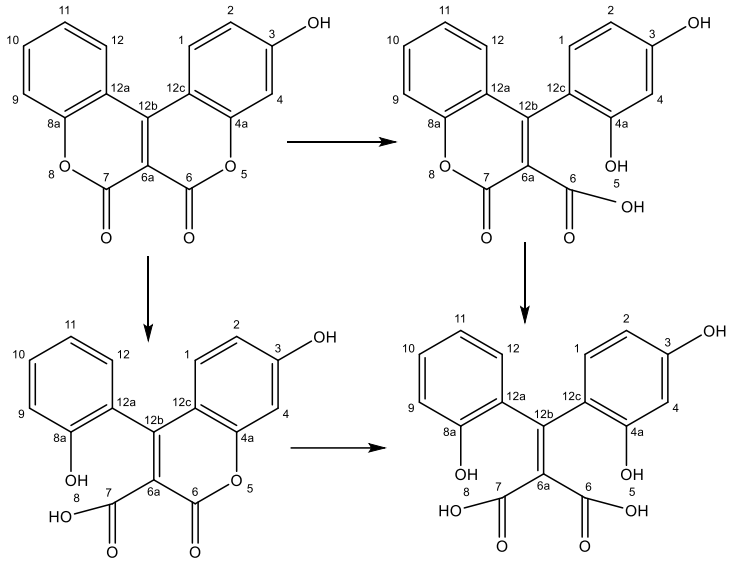

Figure 7. Hypothetical products resulting from hydrolysis of 3-hydroxy-V-coumarin.

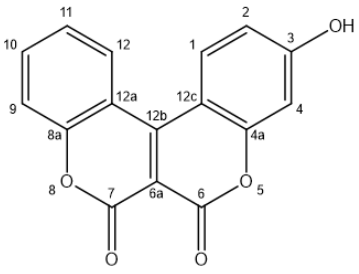

Chemical Formula: $C_{16}H_8O_5$
Exact Mass: 280,03717
Molecular Weight: 280,24
m/z: 280.04 (100.0%), 281.04 (17.3%), 282.04 (1.4%), 282.04 (1.0%)
Elemental Analysis: C, 68.58; H, 2.88; O, 28.55

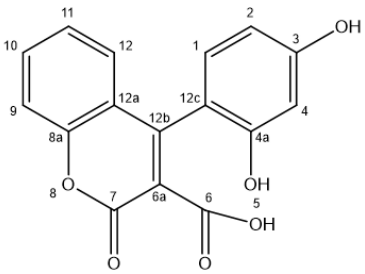

Chemical Formula: $C_{16}H_{10}O_6$
Exact Mass: 298,04774
Molecular Weight: 298,25
m/z: 298.05 (100.0%), 299.05 (17.3%), 300.05 (1.4%), 300.05 (1.2%)
Elemental Analysis: C, 64.43; H, 3.38; O, 32.19

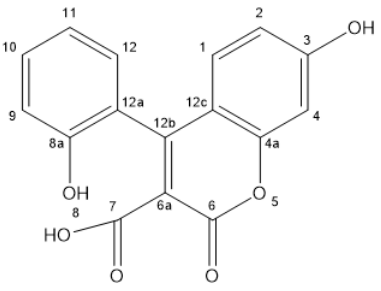

Chemical Formula: $C_{16}H_{10}O_6$
Exact Mass: 298,04774
Molecular Weight: 298,25
m/z: 298.05 (100.0%), 299.05 (17.3%), 300.05 (1.4%), 300.05 (1.2%)
Elemental Analysis: C, 64.43; H, 3.38; O, 32.19

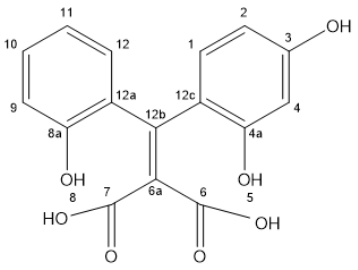

Chemical Formula: $C_{17}H_{14}O_6$
Exact Mass: 314,07904
Molecular Weight: 314,29
m/z: 314.08 (100.0%), 315.08 (18.4%), 316.09 (1.6%), 316.08 (1.2%)
Elemental Analysis: C, 64.97; H, 4.49; O, 30.54

Figure 8. Chemical structure, chemical formula, exact mass, molecular weight, and elemental analysis of 3-hydroxy-V-coumarin and its hypothetical hydrolysis products.

This project also aims to study the effect that pH has on the decrease in fluorescence and confirm that this decrease is dependent on the consumption of 3-hydroxy-V-coumarin in the hydrolysis reaction. The aim is to further investigate whether the formation of hydrolysis products identified through LC-MS analysis correlates with the decrease in 3-hydroxy-V-coumarin fluorescence during the hydrolysis reaction.

Additionally, the objective is to investigate the hydrolysis kinetics of 3-hydroxy-V-coumarin by human liver cytosol and determine kinetic parameters such as Km, Vmax, and intrinsic clearance.

Finally, it is intended to compare the hydrolysis rate of 3-hydroxy-V-coumarin between cytosol of different species such as human, pig, sheep, dog, rabbit, rat, and mouse.

3. Materials and methods

3.1. Chemicals and reagents

3-hydroxy-V-coumarin was provided by Juhani Huuskonen, University of Jyvaskyla. Tris(hydroxymethyl)aminomethane hydrochloride (Tris-HCl), Bio-Rad, and BSA (10mg/mL) were from Sigma-Aldrich. Glycine sodium hydroxide (Glycin-NaOH) was provided by Riedel-de Haën. Calcium chloride ($CaCl_2$) was from MP Biomedicals, LLC. Dimethyl sulfoxide (DMSO) 99.9% and methanol (CH_3OH) optima LC/MS grade were provided by Fisher Chemical. Acetonitrile (CH_3CN) hypergrade was from Merck. Water (H_2O) was deionized by MilliQ gradient A10.

3.2. Biological samples

The male human liver tissue was obtained from Oulu University Hospital in Finland, with approval from the Ethics Committee of the Medical Faculty of the University of Oulu. The pig liver samples were obtained from 8-month-old female pigs utilized for surgical training at Kuopio University. The National Laboratory Animal Centre, Kuopio University provided DBA/2N/Kuo mice (20-25g) and male Wistar rats (200-300g) for the experiments. F. Hoffmann-La Roche Ltd (Nutley, NJ) conducted necropsies on male and female Beagle dogs. Dutch belted rabbits were used in the study, with females aged between 4-11 months and weighing between 2.7-3.8 kg (Licence number: ESAVI/8621/04.10.07/2017). Sheep liver samples were collected from adult female sheep at Oulu University (Oulu, Finland). The collection of liver specimens was approved by the Ethics Committee of the University (Approval No. ESAVI/3510/04.10.03/2011) (42).

3.3. Hydrolysis assays

3.3.1. Assay for the analysis of fluorescence and the hydrolysis metabolites of 3-hydroxy-V-coumarin

3-hydroxy-V-coumarin standards were prepared at concentrations of 0 µM, 0.5 µM, 1 µM, 2.5 µM, and 5 µM in 100 mM Tris-HCl pH 7.4. The composition of the reaction and blank tubes are described in Table 1.

Table 1. Composition of the reaction and blank tubes of the assay 3.3.1.

Reagent	Reaction	Blank	Stock concentrations	Incubation concentrations
Water	335 µL	410 + 10 µL		
Tris-HCl pH 7.4	125 µL	50 µL	400 mM	100 mM
$CaCl_2$	25 µL	25 µL	100 mM	5 mM
3-hydroxy-V-coumarin	5 µL	5 µL	1 mM	10 µM
Rabbit liver cytosol	10 µL	---	16.2 g/L	0.324 g/L

Samples were taken from the reaction and blank tubes, which were being incubated at 37°C, at times: 0 min, 10 min, 20 min, 40 min, and 60 min. These samples were added to tubes containing acetonitrile to stop the reaction, followed by centrifugation (15 minutes at 10,000 x rpm). Supernatant aliquots were pipetted into the wells of a 96 multi-well plate containing 400 mM Tris-HCl at pH 7.4, to be measured by fluorescence and were also pipetted into Eppendorf tubes and stored at -80ºC for subsequent LC-MS analysis.

3.3.2. Assay to confirm the correlation between fluorescence and peak area of 3-hydroxy-V-coumarin and its hydrolysis metabolites

The same assay as in 3.3.1 was conducted but with 2 µM of 3-hydroxy-V-coumarin and a quantity of 1µL of rabbit liver cytosol (0.0162 g/L). Samples were extracted from reaction and blank tubes at times: 0 min, 5 min, 10 min, 15 min, 20 min, 30 min, 40 min, and 60 min. Standard samples of 3-hydroxy-V-coumarin were prepared at concentrations of 0 µM, 0.25 µM, 0.5 µM, 1 µM, and 2 µM, in 100 mM Tris-HCl pH 7.4.

3.3.3. Assay for investigating the impact of pH on hydrolysis of 3-hydroxy-V-coumarin

40 µM 3-hydroxy-V-coumarin was pipetted to the wells of a 96 multi-well plate. Tris-HCl with pHs of 8.2 and 8.6, and Glycin-NaOH with pHs of 9.0, 9.6, 10.0, and 10.6 were pipetted at the same time to the wells that contained 40 µM 3-hydroxy-V-coumarin in the respective order, intended for subsequent fluorescence kinetic measurement.

3.3.4. Assay for the study of hydrolysis kinetics of 3-hydroxy-V-coumarin with human liver cytosol

3-hydroxy-V-coumarin samples were prepared at concentrations of 0 µm, 0.156 µm, 0.313 µm, 0.625 µm, 1.25 µm, 2.5 µm, 5 µm, 10 µm, 20 µm and 40 µm with 10% DMSO and pipetted into three rows of wells on a 96 multi-well plate in the respective order. The composition of the reaction and blank samples are described in Table 2.

Table 2. Composition of the reaction and blank samples of the assay 3.3.4.

Reagent	Reaction	Blank	Stock concentrations	Incubation concentrations
Water	64.8 µL	64.8 + 0.2 µL		
Tris-HCl pH 7.4	25 µL	25 µL	400 mM	100 mM
$CaCl_2$	5 µL	5 µL	100 mM	5 mM
3-hydroxy-V-coumarin	5 µL	5 µL	0.796 mM	Different concentrations
Human liver cytosol	0.2 µL	---	21.6 g/L	0.0432 g/L

Water, Tris-HCl pH 7.4, and $CaCl_2$ in the amounts indicated in Table 2 were pipetted to one row of wells that contained 3-hydroxy-V-coumarin, corresponding to the blank. The same reagents together with human liver cytosol were pipetted to the other two rows of wells that contained 3-hydroxy-V-coumarin, after being heated for 10 minutes at 37°C together with the plate. The reaction aliquots were pipetted at the same time for each well, intended to measure the fluorescence with a kinetic protocol at 37°C.

3.3.5. Assay for investigating the hydrolysis rate of 3-hydroxy-V-coumarin in the cytosol of different species

3-hydroxy-V-coumarin standards were prepared at concentrations of 0 µM, 0.125 µM, 0.25 µM, 0.5 µM, 1 µM and 2 µM with 100mM Tris-HCl pH 7.4. Different cytosol samples from different species were prepared with 100 mM Tris-HCl pH 7.4 and pipetted in a randomized order to the wells of a 96 multi-well plate in duplicate. The composition of the reaction and blank samples are described in Table 3.

Table 3. Composition of the reaction and blank samples of the assay 3.3.5.

Reagent	Reaction	Blank	Stock concentrations	Incubation concentrations
Water	134.5 µL	134.5 + 5 µL		
Tris-HCl pH 7.4	50 µL	50 µL	400 mM	100 mM
$CaCl_2$	10 µL	10 µL	100 mM	5 mM
3-hydroxy-V-coumarin	0.50 µL	0.50 µL	0.796 mM	2 µM
Cytosol	5 µL	---	Different concentrations	Different concentrations

Water, Tris-HCl pH 7.4, $CaCl_2$, and 3-hydroxy-V-coumarin in the amounts indicated in Table 3 were added to the wells that contained the samples of cytosol, after being heated for 5 minutes at 37°C together with the plate, and to another three wells in duplicate, which corresponds with the blank, intended for subsequent fluorescence kinetic measurement.

3.4. Fluorescence measurement

The fluorescence of the samples on the 96 multi-well plates was measured with HIDEX PlateReader SW 1.2, at 444 nm excitation and 520 nm emission wavelengths, 40 times with 30 seconds intervals.

3.5. LC-MS analysis

Before conducting the analytical method, filtration was performed using filters with a diameter of 0.2µm, and syringes of 1mL, after the samples were thawed.

The samples were analyzed by LC-MS using ultra-high performance liquid chromatography equipment (Vanquish Flex UHPLC system, Thermo Scientific, Bremen, Germany) coupled online to high-resolution mass spectrometry equipment (Q Exactive Focus Orbitrap, Thermo Scientific, Bremen, Germany). As the chromatography process was reversed phase, an RP column (Zorbax Eclipse XDBC18, 2.1 × 100mm, 1.8µm, Agilent Technologies, Palo Alto, CA, USA) was maintained at 40°C to inject the sample solutions (2 µL) and run the analysis. The analysis utilized a mobile phase delivered at a flow rate of 400 µL/min, consisting of water (eluent A) and methanol (eluent B), each with 0.1% (v/v) of formic acid. The following gradient profile was used: 0–10 min: 2 to 100% B, 10–14.50 min: 100% B, 14.50–14.51 min: 100 to 2%

B; 14.51–20 min: 2% B. Throughout the analyses, the sample tray was maintained at a temperature of 10°C.

The mass spectrometer was equipped with a heated electrospray ionization source, and data were acquired using the negative ionization mode. The following ESI source settings were employed: a spray voltage of 3.0 kV, sheath gas at a flow rate of 40 (arbitrary units), auxiliary gas at a flow rate of 10 (arbitrary units) and sweep gas at a flow rate of 2 (arbitrary units). Both the capillary and probe heater temperatures were set to 300°C. The detector was calibrated before the sample sequence and operated at high mass accuracy (<2 ppm).

The Orbitrap Q-Exactive spectrometer was employed for data-dependent product ion spectrum (MS^2) experiments, with identical source parameters and chromatography conditions as previously specified. Two scan events were conducted: an MS scan with a specified mass resolution power, and an MS^2 scan in HCD mode, with a normalized collision energy range of 20 to 40%.

3.6. Bradford method – Bio-Rad protein determination

To determine the protein concentration in the cytosol samples of different species, it was used the Bradford method – Bio-Rad protein determination (BioRad, UK).

A Bio-Rad solution (1:5) was prepared and filtered. BSA protein standards were prepared at concentrations of 0 mg/mL, 0.025 mg/mL, 0.05 mg/mL, 0.10 mg/mL, 0.20 mg/mL, 0.40 mg/mL, and 0.80 mg/mL, and then pipetted in duplicate to the wells of a 96 multi-well plate. The cytosol samples and blank samples (with 100mM Tris-HCl pH 7.4) were prepared with a dilution of 1:150 and pipetted to the plate in triplicate. After the Bio-Rad solution (1:5) was pipetted to the plate, a 15-minute incubation period at room temperature was carried out.

The absorbance was measured with HIDEX PlateReader SW 1.2, at 562 nm.

The protein concentration in each cytosol sample was determined using the absorbance values of the samples and the slope (molar extinction coefficient) and y-intercept of the linear regression equation between the absorbance of the BSA standards and their respective concentrations, according to the following equation:

$$Protein\ concentration\ (C) = \frac{Absorbance\ (A) - Y - intercept}{Slope} \quad (1)$$

3.7. Data analysis

3.7.1. LC-MS data analysis

The LC-MS data were analyzed using the Free Style 1.8 software (Thermofisher).

The identification of 3-hydroxy-V-coumarin and its metabolites was based on the retention times, exact mass (*m/z*), and MS^2 spectrum.

The quantification of the compounds was based on the measurement of peak areas. Derived from the peak areas of 3-hydroxy-V-coumarin standards, a calibration curve was plotted as a function of its concentration. The concentrations of 3-hydroxy-V-coumarin at each time point of the reaction were calculated using the peak area values of 3-hydroxy-V-coumarin and the slope and y-intercept of the calibration curve, according to the following equation:

$$Concentration\ (C) = \frac{Peak\ Area\ (PA) - Y - intercept}{Slope} \quad (2)$$

3.7.2. Effect of pH in the hydrolysis of 3-hydroxy-V-coumarin through fluorescence analysis

Data analysis was performed using GraphPad Prism software (Dotmatics).

To determine the relative hydrolysis rate of 3-hydroxy-V-coumarin for each pH (without liver cytosol), it was used the slope of the regressions equations between relative remaining activity (normalized fluorescence values) and incubation time.

The half-life of 3-hydroxy-V-coumarin for each pH was calculated through the analysis of fluorescence over the incubation time using exponential regression.

3.7.3. Hydrolysis kinetics analysis

Data analysis was performed using GraphPad Prism software (Dotmatics).

The concentration of 3-hydroxy-V-coumarin at different time points during the reaction with human liver cytosol was determined using the fluorescence values in those time points and the slopes and y-intercepts of the linear regression equations between the fluorescence of the 3-hydroxy-V-coumarin standards and their respective concentrations, as per the following equation:

$$Concentration\ (C) = \frac{Fluorescence\ (F) - Y - intercept}{Slope} \quad (3)$$

From the regression equations between the concentration of 3-hydroxy-V-coumarin in the reaction and blank samples and the incubation time, the corresponding slopes were extracted. The difference between the slopes of the reaction samples and the blank samples multiplied by the reaction volume corresponds to the ratio between the amount of consumed 3-hydroxy-V-coumarin and time.

The hydrolysis rate of 3-hydroxy-V-coumarin was determined through the following equation:

$$\text{Hydrolysis rate of 3-hydroxy-V-coumarin} = \frac{Amount\ of\ consumed\ 3-hydroxy-V-coumarin}{Time \times Amount\ of\ human\ cytosol\ protein} \quad (4)$$

A Michaelis-Menten analysis relating the hydrolysis rate of 3-hydroxy-V-coumarin with human liver cytosol and its concentration was performed to obtain the kinetic parameters Km and Vmax.

The Michaelis-Menten equation is described below:

$$v = \frac{S \times Vmax}{Km + S} \quad (5)$$

The reaction rate at substrate concentration (S) is denoted by v, while Vmax represents the limiting rate of the reaction. Km is the Michaelis constant, which equals the substrate concentration at which the reaction rate is 50% of Vmax.

The intrinsic clearance corresponds to Vmax/Km.

3.7.4. Enzyme activity analysis

Data analysis was performed using GraphPad Prism software (Dotmatics).

The way in which the concentrations of 3-hydroxy-V-coumarin were determined is described in 3.7.3 according to equation (3).

The enzyme activity was determined through the following equation:

$$\text{Enzyme activity} = \frac{Amount\ of\ consumed\ substrate\ (3{-}hydroxy{-}V{-}coumarin)}{Time \times Amount\ of\ cytosol\ protein} \quad (6)$$

4. Results and discussion

4.1. Analysis of fluorescence during the hydrolysis reaction of 10 µM 3-hydroxy-V-coumarin

After performing an in vitro reaction in the presence of cytosol, substrate decay, and metabolite formation can be detected by fluorometry (23,41). Since 3-hydroxy-V-coumarin exhibits fluorescence (ex 444nm, em 520 nm), measuring its values allows the study of its depletion in the hydrolysis reaction (22).

Figures 9 and 10 illustrate the fluorescence analysis that was performed during the hydrolysis reaction of 10 µM 3-hydroxy-V-coumarin with rabbit liver cytosol (0.324 g/L).

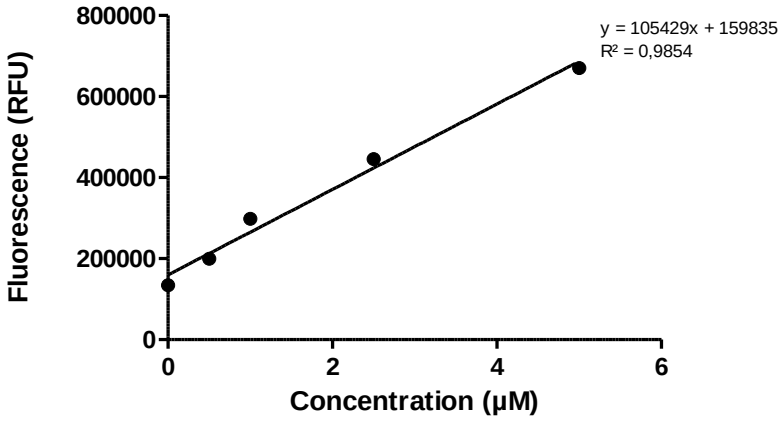

Figure 9. 3-hydroxy-V-coumarin standards linear regression line of the assay 3.3.1.

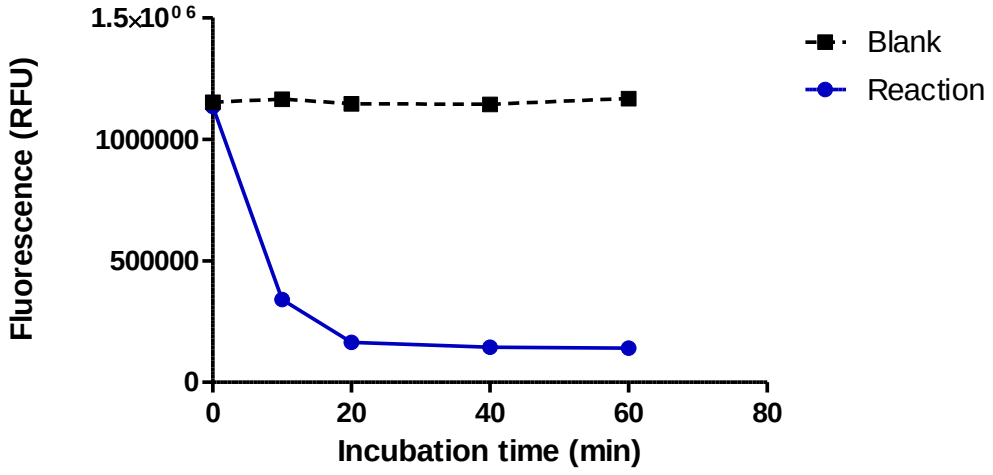

Figure 10. The effect of incubation time on fluorescence of 10 µM 3-hydroxy-V-coumarin.

The fluorescence analysis of 10 µM 3-hydroxy-V-coumarin indicated that the use of rabbit liver cytosol (0.362 g/L) caused an almost complete decrease in fluorescence during the first 20 minutes and remained constant from 20 to 60 minutes (Figure 10), suggesting that the depletion of 10 µM 3-hydroxy-V-coumarin occurred within the first 20 minutes of the reaction.

4.2. LC-MS analysis of 10 µM 3-hydroxy-V-coumarin and its hydrolysis metabolites

Currently, the primary methodologies enabling metabolite analysis include gas chromatography-mass spectrometry (GC–MS), liquid chromatography-mass spectrometry (LC–MS), capillary electrophoresis-mass spectrometry (CE–MS), and nuclear magnetic resonance spectroscopy (NMR). LC-MS methods are currently considered the most versatile analytical approach for detecting and measuring a substrate or its metabolites and present higher selectivity compared to fluorometry (2,23,41). UHPLC–MS offers high sensitivity, selectivity, accuracy, efficiency, and reproducibility, despite being associated with high costs (32,41).

4.2.1. LC-MS analysis of 10 µM 3-hydroxy-V-coumarin

The analysis of LC-MS data enabled the identification of 3-hydroxy-V-coumarin in the standard, blank, and reaction samples. Peaks with an *m/z* value corresponding to the deprotonated molecule of 3-hydroxy-V-coumarin ($[M-H]^-$, *m/z* 279.0299) were detected at a retention time of 6.56 min. Figure 11 illustrates the above, corresponding to the LC-MS chromatogram and mass spectrum of 10 µM 3-hydroxy-V-coumarin in the reaction sample at 0 min.

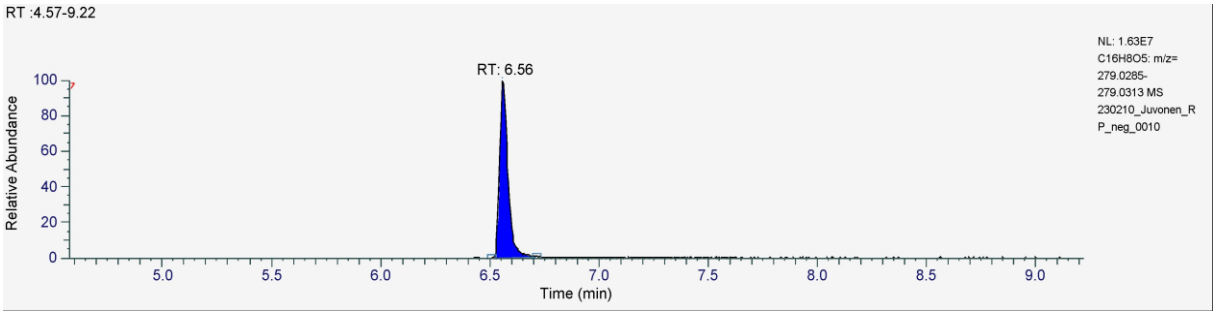

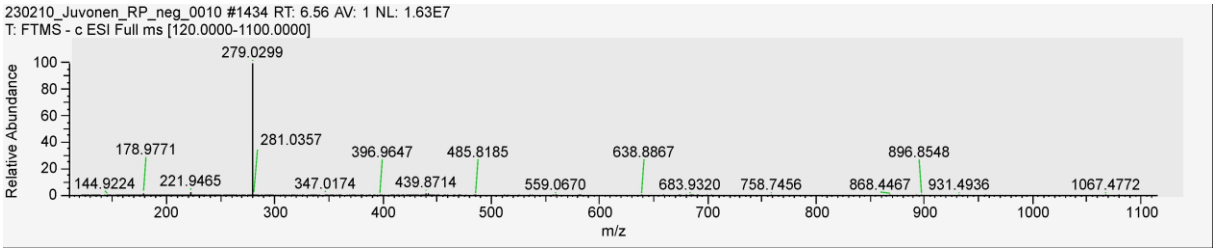

Figure 11. LC-MS chromatogram and mass spectrum of 10 µM 3-hydroxy-V-coumarin in the reaction sample at 0 min.

The LC-MS analysis was also performed with an MS^2 scan on the reaction samples at 0 min and 10 min. Figure 12 illustrates the fragments obtained in the MS^2 spectrum of 10 µM 3-hydroxy-V-coumarin in the reaction sample at 10 min.

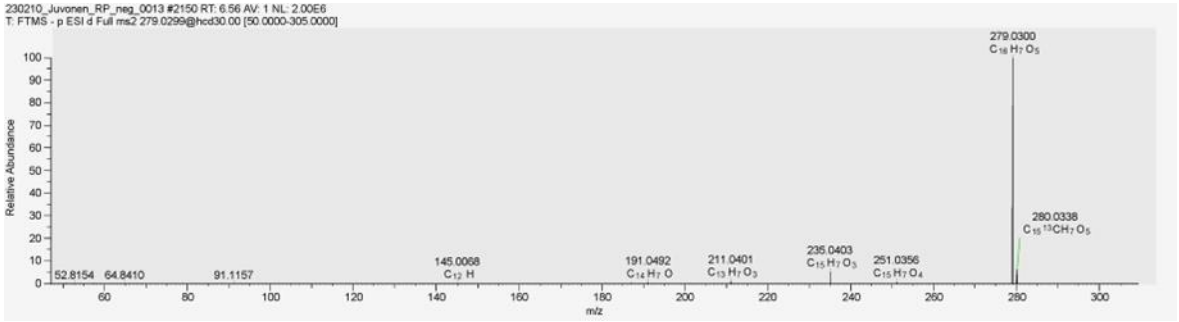

Figure 12. MS^2 spectrum of 10 µM 3-hydroxy-V-coumarin in the reaction sample at 10 min.

In the MS^2 spectrum of 10 µM 3-hydroxy-V-coumarin at the reaction time of 10 minutes shown in Figure 12, it is possible to confirm the presence of the compound in question, as there is not much fragmentation observed and practically only the original compound was detected. The ion of 3-hydroxy-V-coumarin does not easily break in MS/MS due to the ring structure, which makes it very stable.

Figures 14 and 15 aim to illustrate the variation of the peak area and concentration of 10 µM 3-hydroxy-V-coumarin over time during the hydrolysis reaction with rabbit liver cytosol (0.324 g/L).

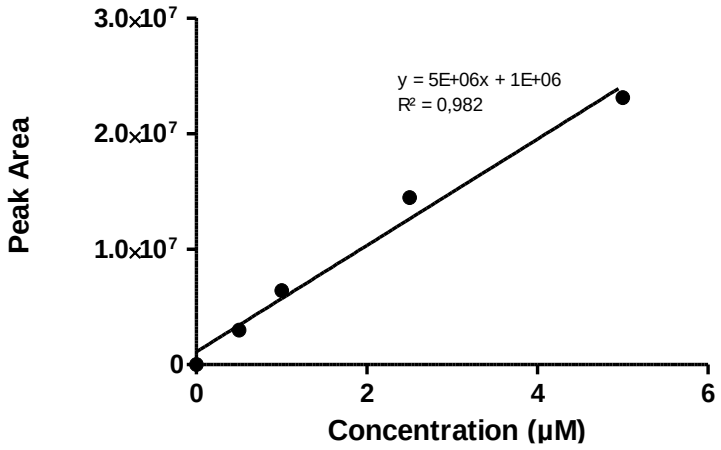

Figure 13. Calibration curve of 3-hydroxy-V-coumarin standards.

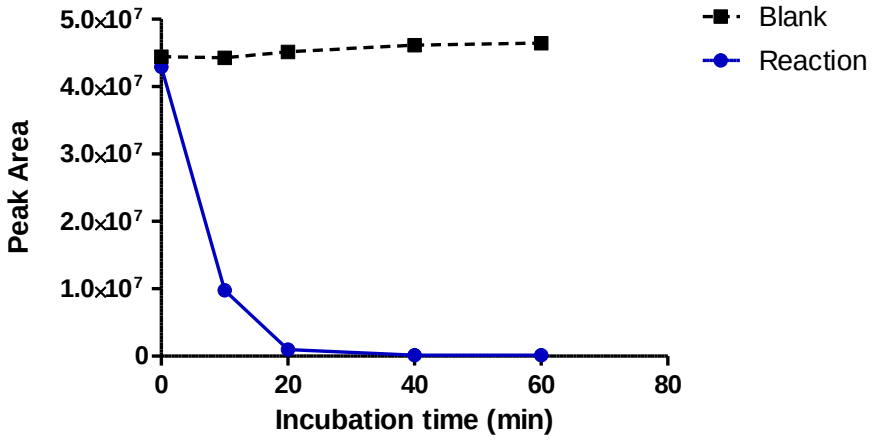

Figure 14. The effect of incubation time on the peak area of 10 µM 3-hydroxy-V-coumarin during the hydrolysis reaction with rabbit liver cytosol (0.324 g/L).

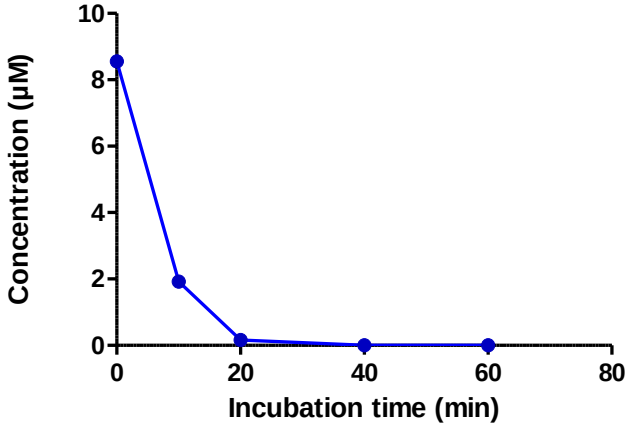

Figure 15. The effect of incubation time on the concentration of 10 µM 3-hydroxy-V-coumarin during the hydrolysis reaction with rabbit liver cytosol (0.324 g/L).

This analysis revealed that the depletion of 10 µM 3-hydroxy-V-coumarin peak area occurred within 20 minutes, as can be seen in Figure 14. This result is consistent with the previously mentioned fluorescence analysis, suggesting that the hydrolysis reaction took place in this period.

Fluorescence and peak areas of 10 µM 3-hydroxy-V-coumarin remained unchanged over time in the blank samples due to the absence of rabbit liver cytosol, which prevented the hydrolysis reaction from occurring, as can be observed in Figure 10 and Figure 14.

4.2.2. LC-MS analysis of 10 µM 3-hydroxy-V-coumarin hydrolysis metabolites

4.2.2.1. LC-MS analysis of $C_{16}H_{10}O_6$

Through analysis of the LC-MS data, two peaks were detected with close retention times (RT=5.76 min and RT=5.85min) and an *m/z* value of 297.0405 only in the reaction samples with rabbit liver cytosol (0.324 g/L) at times 0 min, 10 min, 20 min, 40 min, and 60 min. Figure 16 depicts the aforementioned description, which pertains to the LC-MS chromatogram and mass spectrum of $C_{16}H_{10}O_6$ (RT=5.76 min and RT=5.85 min) in the reaction sample at 40 min.

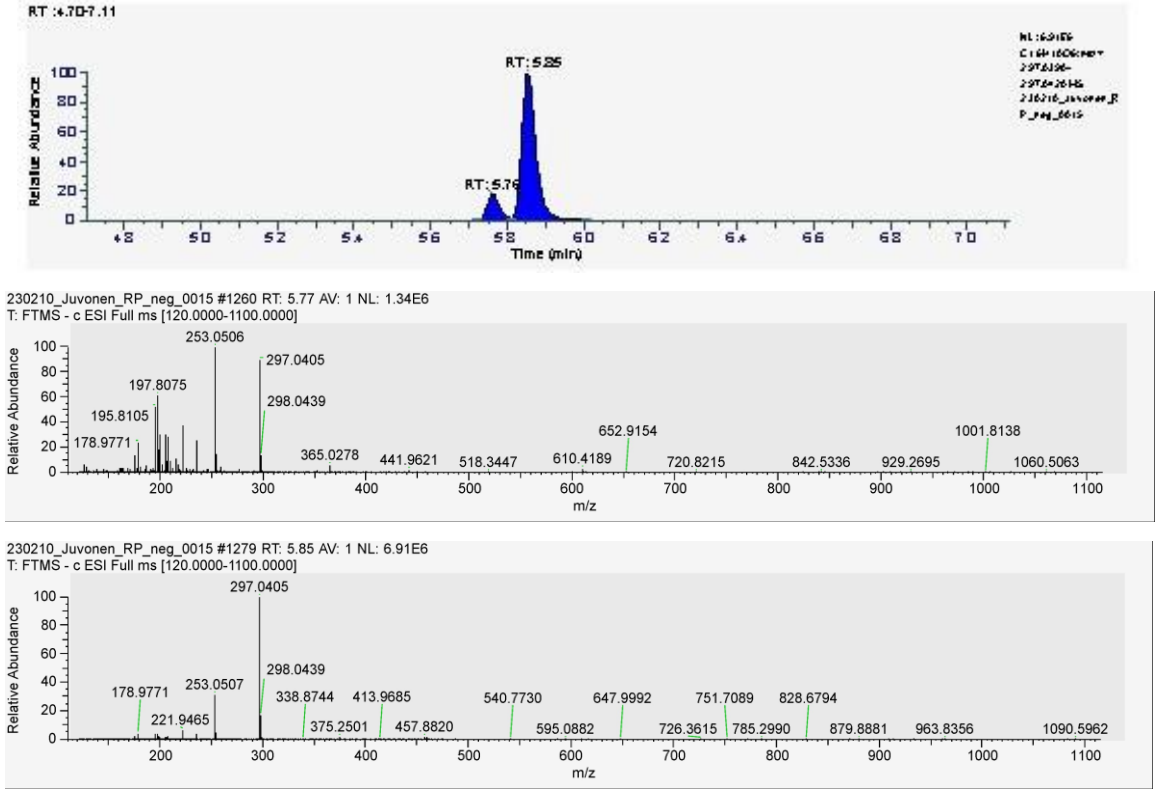

Figure 16. LC-MS chromatogram and mass spectrum of $C_{16}H_{10}O_6$ (RT=5.76 min and RT=5.85min respectively) in the reaction sample at 40 min.

When lactones are hydrolyzed their mass increases by 18 mass units, a change that is easily detected in MS (2). The LC-MS analysis confirmed the formation of 3-hydroxy-V-coumarin metabolites only in the reaction samples. These metabolites resulted from the hydrolysis of only one lactone on each side of 3-hydroxy-V-coumarin since two peaks were detected in the LC-MS spectrum with close retention times (RT = 5.76 min and RT = 5.85 min), corresponding to the deprotonated molecule of $C_{16}H_{10}O_6$ at *m/z* 297.0405 ($[M-H]^-$), like the example shown in Figure 16. The mentioned metabolites are carboxylic acids resulting from lactone hydrolysis $[C_{16}H_8O_5\text{-}H+H20]^-$.

MS/MS data assists in the identification of lactone hydrolysis by providing information about fragmentation patterns (2,40). An MS^2 scan was also used for the LC-MS analysis of the reaction samples at 0 min and 10 min. Figure 17 illustrates the fragments obtained in the MS^2 spectrum of $C_{16}H_{10}O_6$ (RT=5.76 min) in the reaction sample at 10 min.

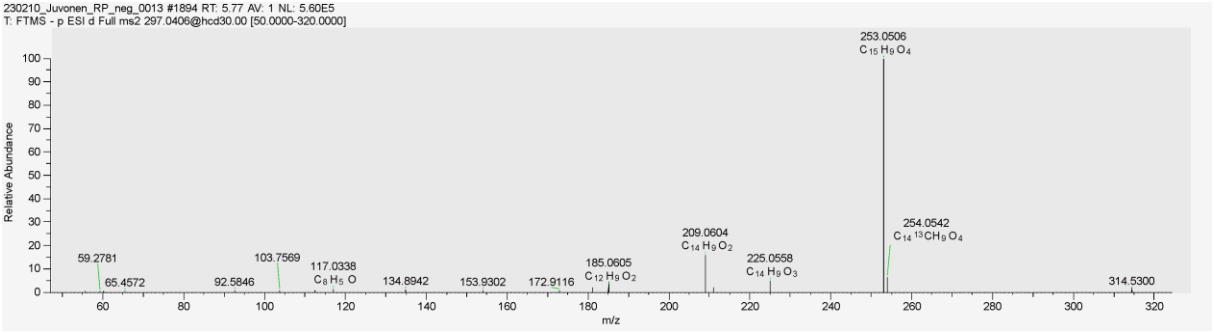

Figure 17. MS^2 spectrum of $C_{16}H_{10}O_6$ (RT=5.76 min) in the reaction sample at 10 min.

In the MS^2 spectrum of $C_{16}H_{10}O_6$ at a reaction time of 10 minutes with a retention time of 5.76 minutes shown in Figure 17, it is evident that there is a significant loss of CO_2 from the parent ion compound since it is labile. This is indicated by the fragment peak with the highest intensity having an *m/z* value of 253.0506, which corresponds to $C_{15}H_9O_4$ ($C_{16}H_9O_6$ - CO_2). The loss of CO_2 is a common occurrence in carboxylic acids, such as the metabolites resulting from the hydrolysis of 3-hydroxy-V-coumarin (2). The hydrolyzed metabolite is highly unstable in MS, and it is not possible to observe the original parent ion with an *m/z* value of 297.0405.

Due to technical reasons in the method setup, it was not possible to observe the MS^2 spectrum of $C_{16}H_{10}O_6$ with a retention time of 5.85 minutes, consequently, it was not feasible to discern which metabolite elutes first and which metabolite elutes later.

Figures 18 and 19, and Table 4 aim to illustrate the variation of the peak area of the metabolites $C_{16}H_{10}O_6$ (RT=5.76 min and RT=5.85min) over time during the hydrolysis reaction with rabbit liver cytosol (0.324 g/L).

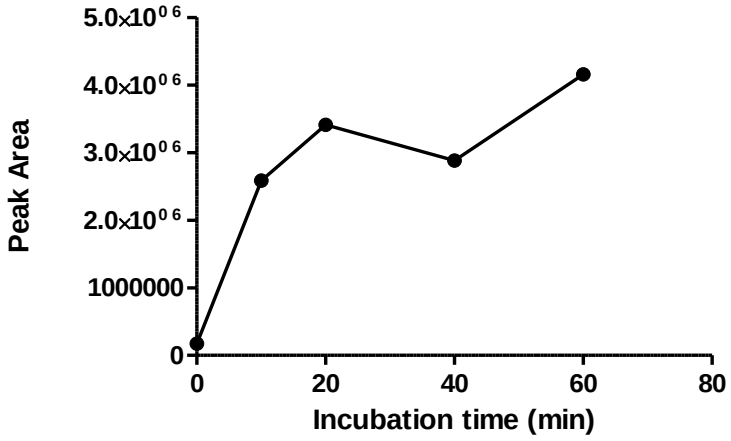

Figure 18. Peak area variation over time of $C_{16}H_{10}O_6$ with RT= 5.76 min during the hydrolysis reaction with rabbit liver cytosol (0.324 g/L).

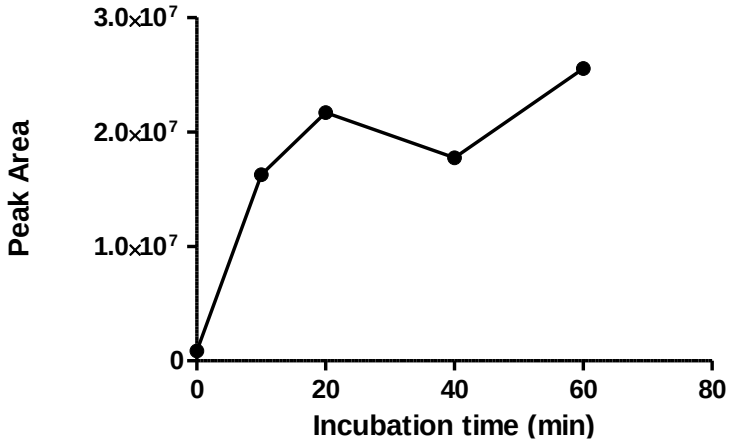

Figure 19. Peak area variation over time of $C_{16}H_{10}O_6$ with RT= 5.85 min during the hydrolysis reaction with rabbit liver cytosol (0.324 g/L).

The peak areas of these metabolites experienced a more significant increase within the first 20 minutes of the hydrolysis reaction, as can be observed in Figure 18 and Figure 19.

Table 4. Peak areas of the metabolites $C_{16}H_{10}O_6$ with RT = 5.76 min and RT = 5.85 min of the hydrolysis reaction with rabbit liver cytosol (0.324 g/L).

Time (min)	Peak area $C_{16}H_{10}O_6$ RT = 5.76 min	Peak area $C_{16}H_{10}O_6$ RT = 5.85 min	Metabolites peak areas ratio
0	171,841.09	866,385.45	5.0
10	2,583,643.77	16,271,475.20	6.3
20	3,412,488.55	21,675,229.06	6.4
40	2,881,647.12	17,734,476.69	6.2
60	4,155,201.65	25,543,420.37	5.0

These metabolites did not form in equal amounts: the metabolite $C_{16}H_{10}O_6$ with RT = 5.85 min is formed 5- to 6-fold times more than the metabolite $C_{16}H_{10}O_6$ with RT = 5.76 min, as described in Table 4.

4.2.2.2. LC-MS analysis of $C_{17}H_{14}O_6$

There were no peaks detected with the retention time and *m/z* value corresponding to the deprotonated molecule of $C_{17}H_{14}O_6$ (313.0718). Therefore, it can be concluded that the metabolite corresponding to two consecutive hydrolyses of the two lactones of 3-hydroxy-V-coumarin was not formed.

4.3. Correlation between LC-MS analysis and fluorescence of 2 µM 3-hydroxy-V-coumarin and its hydrolysis metabolites

To confirm the correlation between the peak area and fluorescence of 3-hydroxy-V-coumarin and between peak area and decrease in fluorescence of 3-hydroxy-V-coumarin hydrolysis metabolites, another LC-MS analysis was performed with more time points and using fewer amount of rabbit liver cytosol, to obtain a slower reaction.

The LC-MS analysis of the incubation samples with 2 µM 3-hydroxy-V-coumarin and rabbit liver cytosol (0.0162g/L) revealed the presence of peaks with the same retention time and *m/z* value as those described in 4.2.2. The ratios between the peak areas of $C_{16}H_{10}O_6$ with RT = 5.85

min and RT = 5.76 min at times 0 min, 5 min, 10 min, 15 min, 20 min, 30 min, 40 min, and 60 min varied between 5 and 6. In essence, this analysis revealed the formation of the same hydrolysis metabolites and in the same proportion as in the previously mentioned LC-MS analysis. Figure 20 summarizes the metabolites obtained from the hydrolysis of 3-hydroxy-V-coumarin with rabbit liver cytosol.

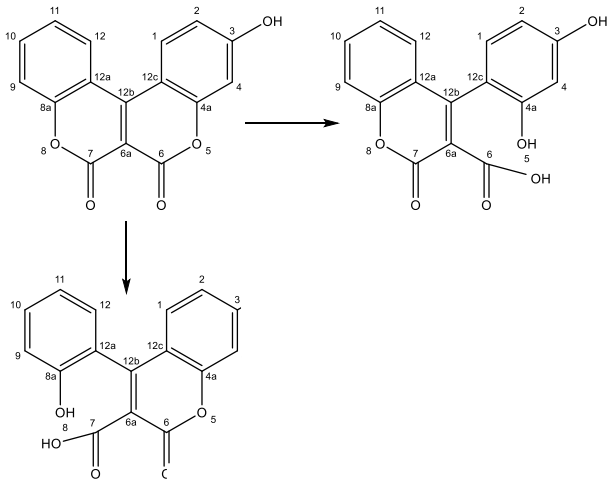

Figure 20. Metabolites obtained from the hydrolysis of 3-hydroxy-V-coumarin with rabbit liver cytosol.

4.3.1. Correlation between peak area and fluorescence of 2 µM 3-hydroxy-V-coumarin

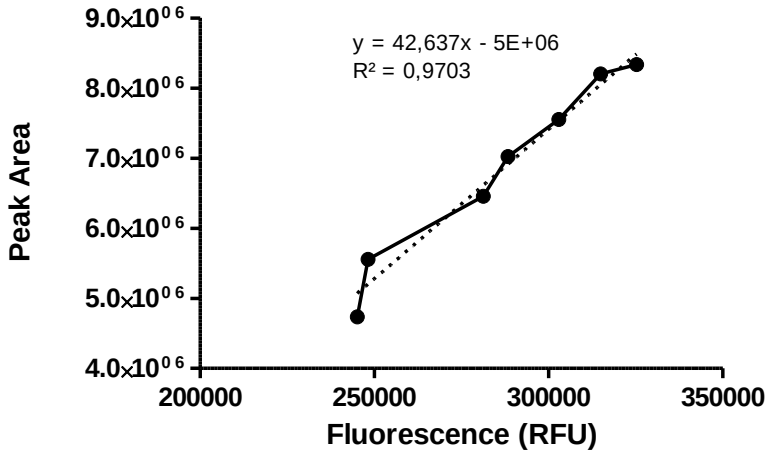

Figure 21. Correlation between peak area of 2 µM 3-hydroxy-V-coumarin and fluorescence during the hydrolysis reaction with rabbit liver cytosol (0.0162g/L).

4.3.2. Correlation between peak area and decrease in fluorescence of 2 µM 3-hydroxy-V-coumarin hydrolysis metabolites

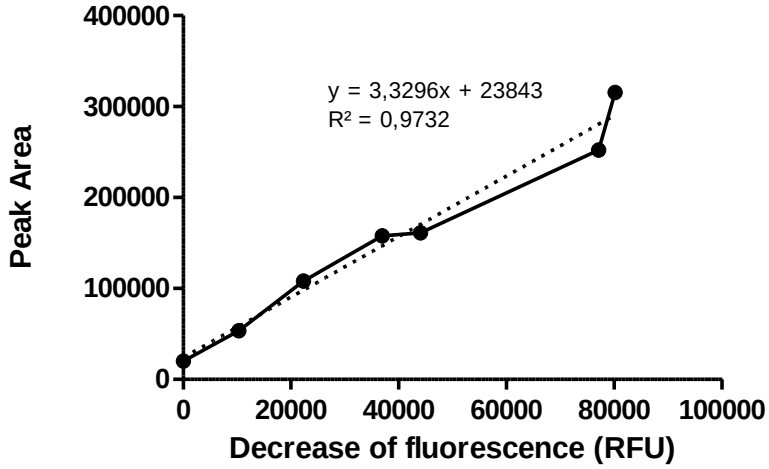

Figure 22. Correlation between peak area of $C_{16}H_{10}O_6$ with RT= 5.76 and decrease in fluorescence during the hydrolysis reaction with rabbit liver cytosol (0.0162g/L).

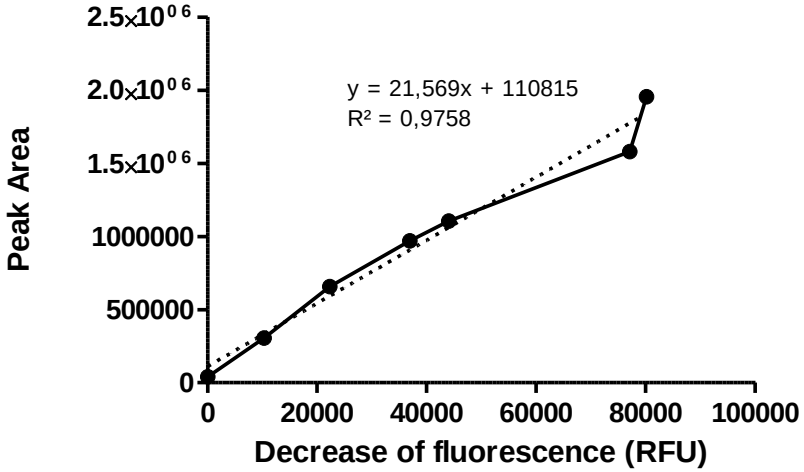

Figure 23. Correlation between peak area of $C_{16}H_{10}O_6$ with RT= 5.85 and decrease in fluorescence during the hydrolysis reaction with rabbit liver cytosol (0.0162g/L).

In both the fast reaction, with a higher concentration of rabbit liver cytosol (0.324 g/L), and the slow reaction, with a lower concentration of rabbit liver cytosol (0.0162 g/L) there is an approximately linear correlation between peak area and fluorescence of 3-hydroxy-V-coumarin, as shown in Figure 21. The same applies to peak area and the decrease in fluorescence of the 3-hydroxy-V-coumarin hydrolysis metabolites formed - $C_{16}H_{10}O_6$ with RT = 5.76 min and $C_{16}H_{10}O_6$ with RT = 5.85 min, as shown in Figure 22 and Figure 23. The 60-minute time point was removed as it constituted an outlier due to the presence of an artifact.

With this analysis, it is confirmed that the decrease in fluorescence of 3-hydroxy-V-coumarin is related to its depletion during the hydrolysis reaction and with the formation of non-fluorescent (at 444 nm excitation and 520 nm emission wavelengths) 3-hydroxy-V-coumarin metabolites corresponding to the hydrolysis of only one lactone.

4.4. The effect of pH on hydrolysis of 3-hydroxy-V-coumarin

To examine the effect of pH on the hydrolysis reaction of 3-hydroxy-V-coumarin, the fluorescence at pHs 8.2, 8.6, 9.0, 9.2, 9.6, 10.0, 10.3, and 10.6 were analyzed. The following figures (24, 25, 26, and 27) illustrate the effect of pH on the fluorescence and hydrolysis of 3-hydroxy-V-coumarin.

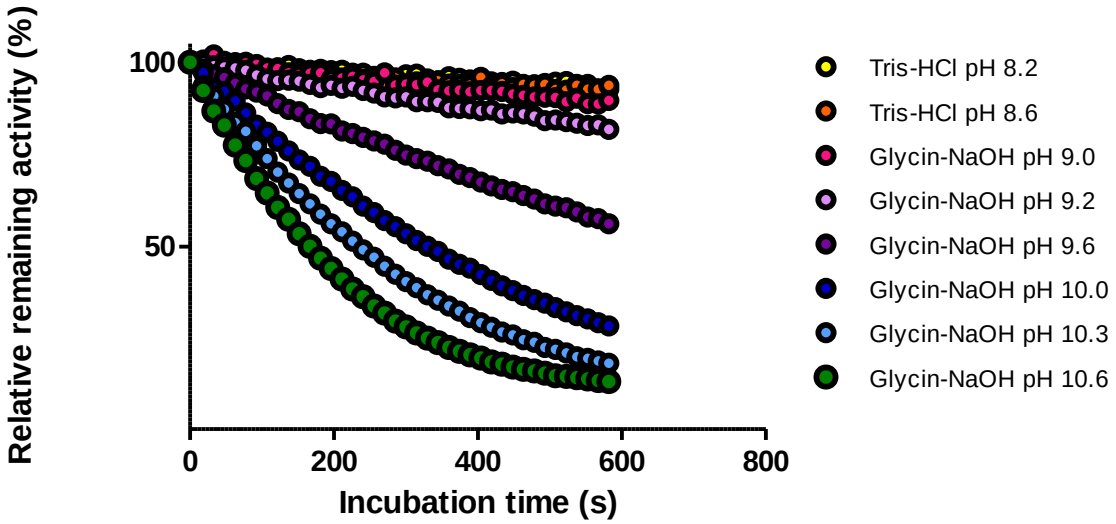

Figure 24. Relative remaining activity of 3-hydroxy-V-coumarin over time.

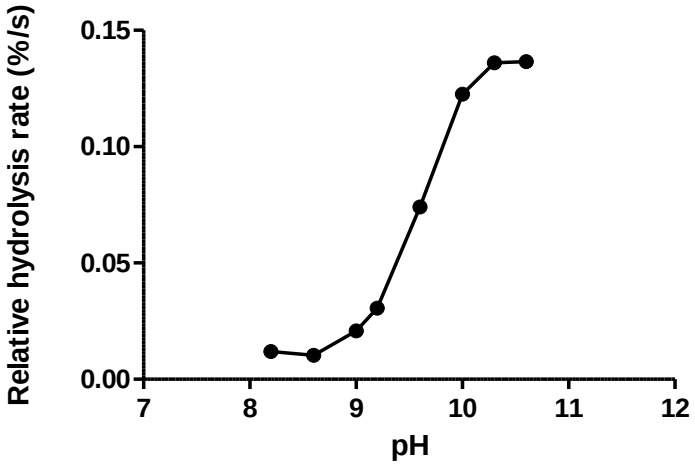

Figure 25. Relative hydrolysis rate of 3-hydroxy-V-coumarin in different pHs.

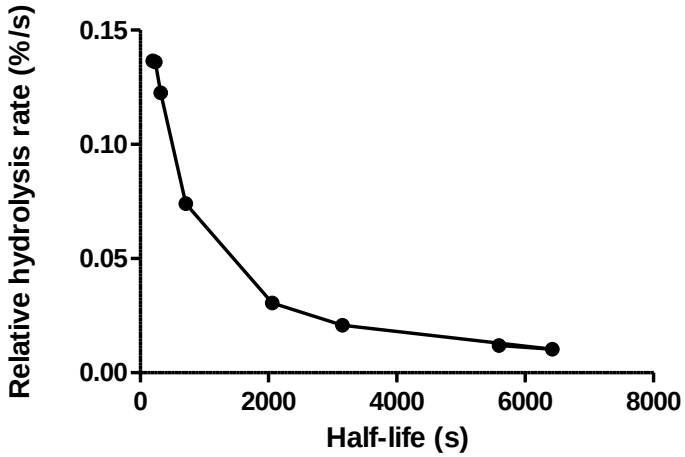

Figure 26. Relative hydrolysis rate of 3-hydroxy-V-coumarin as a function of its half-life.

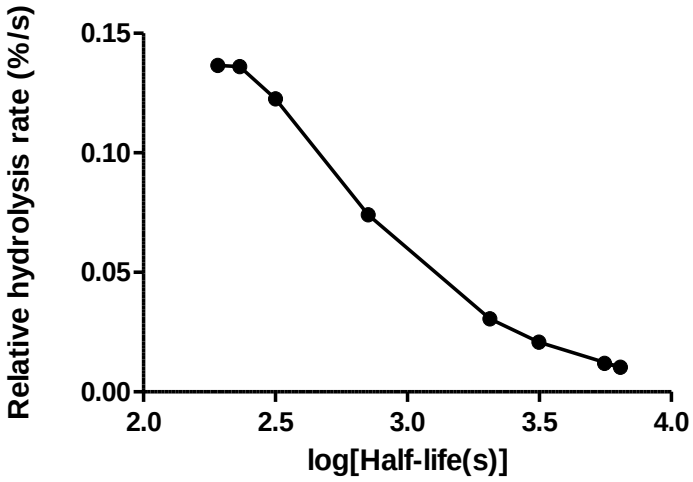

Figure 27. Relative hydrolysis rate of 3-hydroxy-V-coumarin as a function of the logarithm of its half-life.

According to Figure 24 and Figure 25, the fluorescence of 3-hydroxy-V-coumarin was stable in pHs under 9.0, and there was a rapid decline in the fluorescence from that pH onwards due to hydrolysis, revealing that the spontaneous hydrolysis reaction (without liver cytosol) only takes place over pH 9. At pHs 8.2 and 8.6, 40µM 3-hydroxy-V-coumarin did not hydrolyze. From pH 10, there is no longer any reaction due to substrate consumption. This analysis proved that the rate of the spontaneous hydrolysis reaction is pH dependent. It was also proven that as the half-life of 3-hydroxy-V-coumarin increases, the relative hydrolysis rate decreases, as can be observed in Figure 26. This analysis confirms that 3-hydroxy-V-coumarin undergoes spontaneous hydrolysis under alkaline pH, in addition to enzymatic hydrolysis.

4.5. Hydrolysis kinetics of 3-hydroxy-V-coumarin in human liver cytosol

The figures below (28, 29, 30, and 31) aim to illustrate the study of the hydrolysis kinetics of 3-hydroxy-V-coumarin with human liver cytosol (0.0432 g/L).

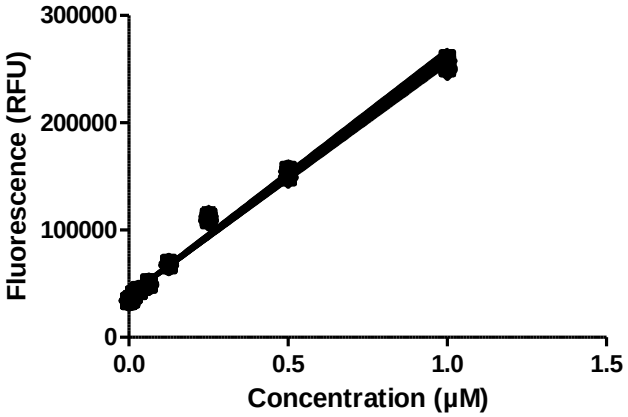

Figure 28. 3-hydroxy-V-coumarin standards linear regression lines of the assay 3.3.4.

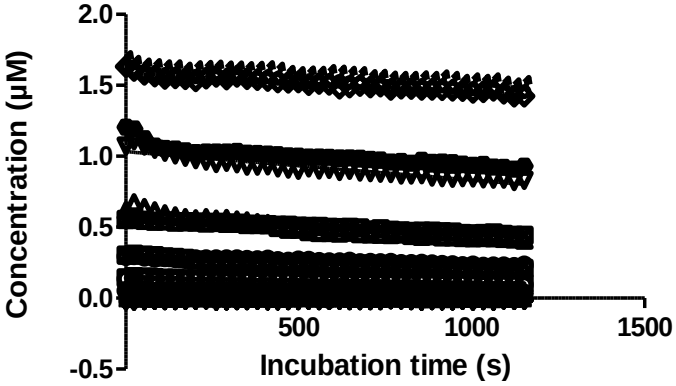

Figure 29. The effect of the concentration of 3-hydroxy-V-coumarin on its concentration decrease during the hydrolysis reactions with human liver cytosol (0.0432 g/L).

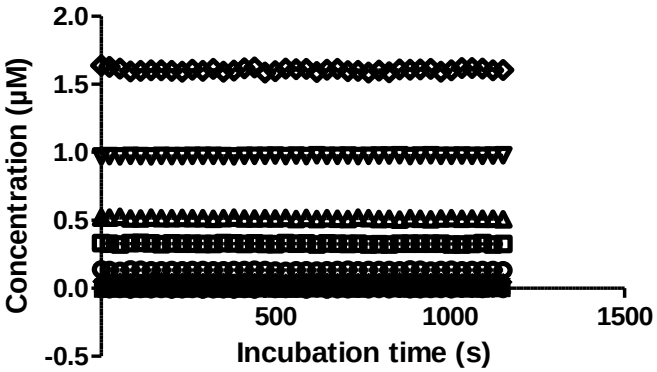

Figure 30. The effect of the concentration of 3-hydroxy-V-coumarin on its concentration decrease in the blank samples.

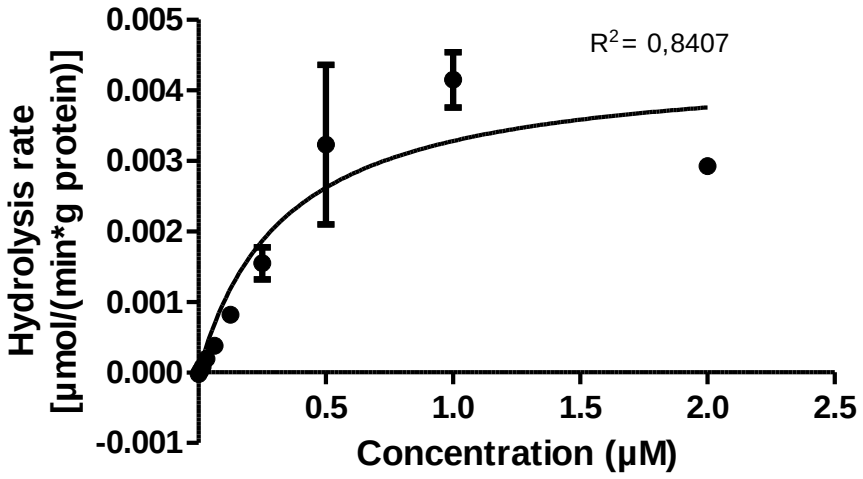

Figure 31. Michaelis-Menten analysis of the hydrolysis reaction of 3-hydroxy-V-coumarin with human liver cytosol (0.0432 g/L).

Table 5 aims to illustrate the best-fit values and 95% confidence intervals for the kinetic parameters of the hydrolysis reaction of 3-hydroxy-V-coumarin with human liver cytosol (0.0432 g/L).

Table 5. Kinetic parameters of the hydrolysis reaction of 3-hydroxy-V-coumarin with human liver cytosol (0.0432 g/L).

Vmax [(nmol/(min*g protein)]	**Km (nM)**	**Intrinsic clearance [L/(min*g protein)]**
4.40 (3.05 to 5.74)	340.0 (40.8 to 639.3)	0.0129

Human liver cytosol was used to determine the kinetic parameters of the 3-hydroxy-V-coumarin hydrolysis reaction, which can be consulted in Table 5. Through Figure 29, it is possible to observe that the concentration of 3-hydroxy-V-coumarin decreases over time in the presence of human liver cytosol, in contrast to what happens in the blank samples, where the concentration of 3-hydroxy-V-coumarin does not change since human liver cytosol is absent, as can be seen in Figure 30. This decrease in the concentration of 3-hydroxy-V-coumarin is the result of its consumption in the hydrolysis reaction catalyzed by enzymes present in the human liver cytosol. Given the relatively high value of R-squared of the Michaelis-Menten analysis, represented in Figure 31, it is likely that a single enzyme found in the cytosol of the human liver is responsible for catalyzing the hydrolysis reaction. Alternatively, it could be more than one enzyme from the same family or with the same enzymatic kinetics. Considering that the structure of 3-hydroxy-V-coumarin contains two lactones, it is probable that an enzyme of the PON family is responsible for its hydrolysis, however, further studies are needed to confirm.

4.6. Protein concentration in the cytosol of different species.

Figure 32 and Table 6 correspond to the results obtained through the Bradford method – Bio-Rad protein determination, with the purpose to be used in the study of the hydrolysis rate in the cytosol of different species.

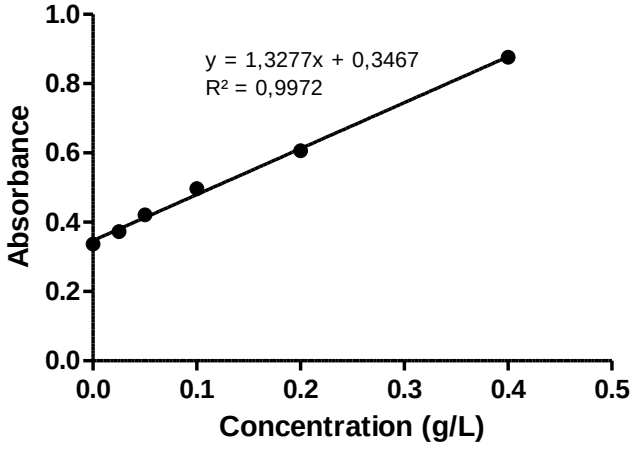

Figure 32. BSA standards linear regression line.

Table 6. Absorbance and protein concentration values of liver cytosol samples of different species.

Species	Absorbance	Protein concentration (g/L)
Mouse 1	0.588	27.3
Mouse 2	0.630	32.0
Mouse 3	0.584	26.8
Mouse 4	0.630	32.0
Mouse 5	0.622	31.1
Human (HL-15)	0.482	15.3
Human (HL-22)	-	23.4
Sheep 6	-	22.5
Sheep 11	-	26.7
Sheep 17	-	22.0
Sheep 89	-	21.4
Sheep 93	-	16.4
Rabbit 4	-	26.1
Rabbit 5	-	31.0
Rabbit 6	-	25.9
Rabbit 7	-	23.1
Rabbit 8	-	21.4
Dog 1	-	18.3
Dog 2	-	27.5
Dog 3	-	28.4
Dog 7	-	29.8
Dog 8	-	23.8
Dog 9	-	24.1
Pig 4	-	28.0
Pig 5	-	26.8
Pig 7	-	23.1
Pig 8	-	23.4
Pig 10	-	19.4
Pig 11	-	23.7
Rat 1	-	18.3

Rat 2	-	20.7
Rat 3	-	18.8
Rat 4	-	16.1
Rat 5	-	19.2
Mouse control female	-	18.3
Mouse control male	-	18.8
Mouse phenobarbital female	-	22.3
Mouse phenobarbital male	-	21.1

Certain liver cytosol samples lack an absorption value in Table 5 because their concentrations were determined earlier.

4.7. Hydrolysis rate of 3-hydroxy-V-coumarin in the cytosol of different species

Figures 34, 35, and 36 illustrate the study of the hydrolysis rate of 3-hydroxy-V-coumarin in the liver cytosol of different species.

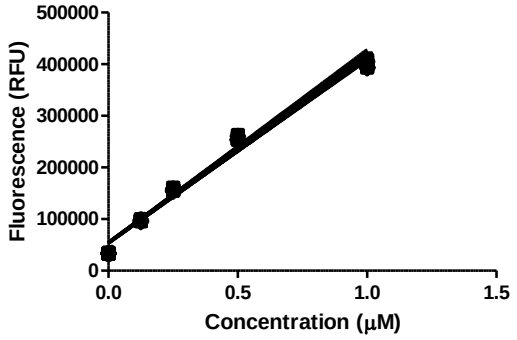

Figure 33. 3-hydroxy-V-coumarin standards linear regressions lines of the assay 3.3.5.

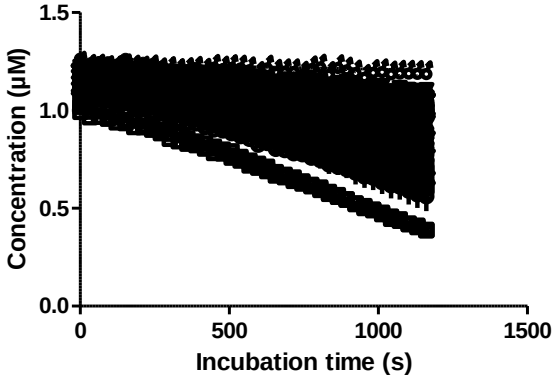

Figure 34. The effect of incubation on the concentration of 3-hydroxy-V-coumarin during the hydrolysis reactions with liver cytosol of different species.

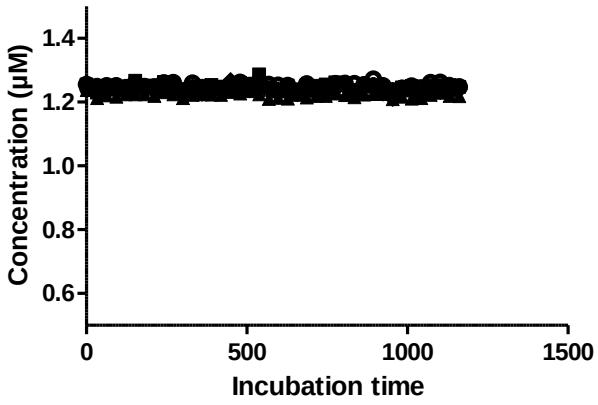

Figure 35. The effect of incubation on the concentration of 3-hydroxy-V-coumarin in the blank samples.

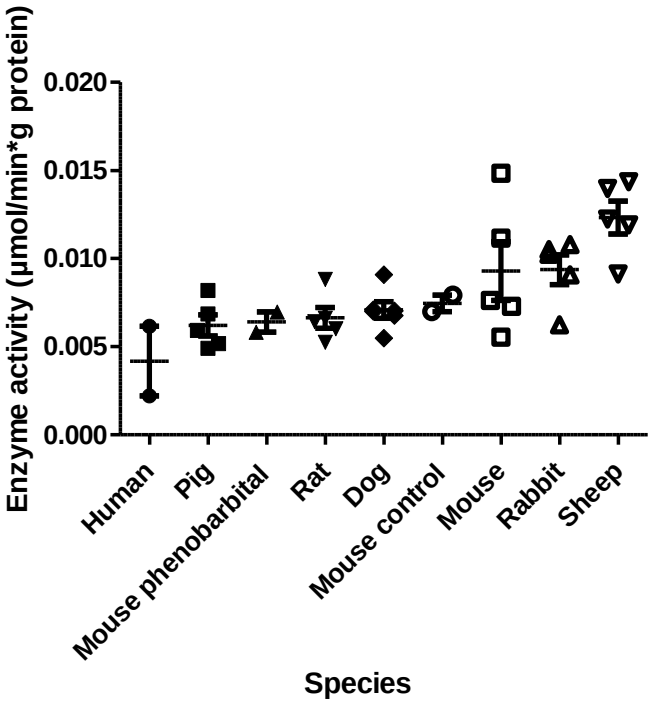

Figure 36. Enzyme activity in the hydrolysis reaction of 3-hydroxy-V-coumarin with liver cytosol of different species.

To determine the hydrolysis rate of 3-hydroxy-V-coumarin in the liver cytosol of different species, multiple samples of each species were used. Through Figure 34, it is possible to observe that the concentration of 3-hydroxy-V-coumarin decreases in all samples containing liver cytosol from different species, in contrast to what happens in the blank samples, as can be seen in Figure 35. The reduction in the concentration of 3-hydroxy-V-coumarin is due to its consumption in the hydrolysis reaction, which is facilitated by enzymes that are present in the

liver cytosol of the studied species. The results showed that 3-hydroxy-V-coumarin is hydrolyzed in all the studied species, however, there are differences in the hydrolysis rate inter- and intra-species. Based on the conducted analysis, sheep exhibited the highest rate of hydrolysis of 3-hydroxy-V-coumarin, followed by rabbit, mouse, mouse control, dog, rat, mouse phenobarbital, pig, and human in descending order, as can be observed in Figure 36. The lower enzymatic activity observed in the mouse treated with phenobarbital compared to the control mouse indicates that phenobarbital is not an effective inducer for the enzyme responsible for the hydrolysis of 3-hydroxy-V-coumarin, as it is for CYP 450 enzymes (43).

5. Conclusion

Given the importance of studying drug metabolism in the early stages of its development to exclude potentially toxic or ineffective candidates, it was investigated the 3-hydroxy-V-coumarin metabolism, specifically focusing on the hydrolysis reaction that was expected based on the chemical structure of this compound. In addition to 3-hydroxy-V-coumarin belonging to the group of coumarins, which already possess therapeutic potential in numerous diseases, this compound is part of the π-expanded coumarins, which have distinctive properties, making them an appealing subject of study.

3-hydroxy-V-coumarin exhibits fluorescence enabling the realization of fluorometric analysis, which revealed its consumption in the presence of rabbit liver cytosol. Liquid chromatography coupled with mass spectrometry also revealed the depletion of this compound in the same conditions, verified by the reduction in peak area, so it was concluded an approximately linear correlation between peak area and fluorescence of 3-hydroxy-V-coumarin, that is, a concordance between the fluorometry and LC-MS analyses in two distinct reactions each involving different concentrations of rabbit liver cytosol, and consequently different reaction rates.

The same LC-MS analyses, conducted in both full scan and MS^2 scan modes, enabled the identification of metabolites resulting from the hydrolysis of a lactone on each side of the 3-hydroxy-V-coumarin molecule. For technical reasons, it was not possible to correlate these metabolites with the observed retention times. An approximately linear correlation was observed between the peak area and the decrease in fluorescence of the 3-hydroxy-V-coumarin hydrolysis metabolites formed. It is thus concluded that the depletion of 3-hydroxy-V-coumarin fluorescence and peak area (in the presence of rabbit liver cytosol) is explained by its consumption during the hydrolysis reaction and the formation of non-fluorescent metabolites.

From the analysis of the influence of pH on the occurrence of spontaneous hydrolysis of 3-hydroxy-V-coumarin, it was concluded that pH significantly impacts the rate of this reaction since 3-hydroxy-V-coumarin only underwent hydrolysis from pH 9.

The conducted Michaelis-Menten analysis allowed the determination of the hydrolysis reaction kinetic parameters of 3-hydroxy-V-coumarin in the presence of human liver cytosol, including

a Vmax of 4.40 (3.05 to 5.74) nmol/(min*g protein); a Km of 340.0 (40.8 to 639.3) nM; and an Intrinsic clearance of 0.0129 L/(min*g protein).

Through an investigation into the hydrolysis rate of 3-hydroxy-V-coumarin with cytosol from different species, it was concluded that differences exist in both inter- and intra-species. Among the species tested, sheep exhibit the highest hydrolysis rate. It was also concluded that phenobarbital does not function as an enzymatic inducer for the enzymes responsible for the hydrolysis of 3-hydroxy-V-coumarin. This is evident as, when comparing a control mouse with a mouse treated with phenobarbital, the latter exhibited lower enzymatic activity.

A future repetition of the LC-MS analysis, with improved technical parameters, will be required to obtain the MS^2 spectrum of the hydrolysis metabolite that could not be obtained in this project. This will facilitate the distinction between the two metabolites that have been formed during the hydrolysis reaction.

Continuing research on the metabolism of 3-hydroxy-V-coumarin is crucial, as studies on sulfonation and glucuronidation reactions are also underway. Future studies also include the use of docking tools to investigate whether 3-hydroxy-V-coumarin serves as a substrate for any enzymes in the PON family. It is believed that one or more enzymes from this family might be responsible for the hydrolysis of this compound.

Prospects involve the identification of all metabolites that can be formed from 3-hydroxy-V-coumarin, assessing their toxicity, and exploring potential pharmacological effects that may come from these metabolites or the original compound, with therapeutic and diagnostic potential in mind, or other potential applications that may arise, such as environmental detection or biosensors.

6. References

1. Barba-Ostria C, Carrera-Pacheco SE, Gonzalez-Pastor R, Heredia-Moya J, Mayorga-Ramos A, Rodríguez-Pólit C, et al. Evaluation of Biological Activity of Natural Compounds: Current Trends and Methods. Molecules. 2022 Jul 13;27(14):4490.
2. Yi L, Bandu ML, Desaire H. Identifying lactone hydrolysis in pharmaceuticals. A tool for metabolite structural characterization. Anal Chem. 2005 Oct 15;77(20):6655–63.
3. Carneiro A, Matos MJ, Uriarte E, Santana L. Trending topics on coumarin and its derivatives in 2020. Molecules. 2021 Jan 19;26(2):501.
4. Currie GM. Pharmacology, part 2: Introduction to pharmacokinetics. J Nucl Med Technol. 2018 Sep 1;46(3):221–230.
5. Zhang Z, Tang W. Drug metabolism in drug discovery and development. Acta Pharm Sin B. 2018 Sep;8(5):721-732.
6. Benedetti MS, Whomsley R, Poggesi I, Cawello W, Mathy FX, Delporte ML, et al. Drug metabolism and pharmacokinetics. Drug Metab Rev. 2009;41(3):344-90.
7. Almazroo OA, Miah MK, Venkataramanan R. Drug Metabolism in the Liver. Clin Liver Dis. 2017 Feb;21(1):1-20.
8. Fukami T, Yokoi T, Nakajima M. Non-P450 Drug-Metabolizing Enzymes: Contribution to Drug Disposition, Toxicity, and Development. Annu Rev Pharmacol Toxicol. 2022 Jan 6;62:405-425.
9. van den Anker J, Reed MD, Allegaert K, Kearns GL. Developmental Changes in Pharmacokinetics and Pharmacodynamics. J Clin Pharmacol. 2018 Oct 1;58:S10–25.
10. Sahi J, Grepper S, Smith C. Hepatocytes as a Tool in Drug Metabolism, Transport and Safety Evaluations in Drug Discovery. Curr Drug Discov Technol. 2010 Sep;7(3):188-98.
11. Kulsharova G, Kurmangaliyeva A. Liver microphysiological platforms for drug metabolism applications. Cell Prolif. 2021 Sep;54(9):e13099.
12. Parkinson A, Ogilvie BW, Buckley DB, Kazmi F, Parkinson O. Casarett & Doull's Toxicology: The Basic Science of Poisons. Biotransformation of Xenobiotics. 2015;6(9):223-1.

13. Gómez-Bombarelli R, Calle E, Casado J. Mechanisms of lactone hydrolysis in neutral and alkaline conditions. Journal of Organic Chemistry. 2013 Jul 19;78(14):6868–79.

14. Mohammed CJ, Lamichhane S, Connolly JA, Soehnlen SM, Khalaf FK, Malhotra D, et al. A PON for All Seasons: Comparing Paraoxonase Enzyme Substrates, Activity and Action including the Role of PON3 in Health and Disease. Antioxidants (Basel). 2022 Mar 19;11(3):590.

15. Furlong CE, Marsillach J, Jarvik GP, Costa LG. Paraoxonases-1, -2 and -3: What are their functions? Chem Biol Interact. 2016 Nov 25;259:51–62.

16. Akkol EK, Genç Y, Karpuz B, Sobarzo-Sánchez E, Capasso R. Coumarins and coumarin-related compounds in pharmacotherapy of cancer. Cancers (Basel). 2020 Jul 19;12(7):1959.

17. Wagner BD. The use of coumarins as environmentally-sensitive fluorescent probes of heterogeneous inclusion systems. Molecules. 2009 Jan 6;14(1):210-37.

18. Khemakhem S, Elleuch S, Ben Azaza N, Ammar H, Abid Y. Hydrolysis and substitution effects on the optical properties of coumarin derivatives studied by vibrational spectroscopy and DFT calculation. Journal of Molecular Structure. Elsevier B.V. 2018;1168:65–72.

19. Flores-Morales V, Villasana-Ruíz AP, Garza-Veloz I, González-Delgado S, Martinez-Fierro ML. Therapeutic Effects of Coumarins with Different Substitution Patterns. Molecules. 2023 Mar 6;28(5):2413.

20. Jiang X, Shangguan M, Lu Z, Yi S, Zeng X, Zhang Y, et al. A “turn-on” fluorescent probe based on V-shaped bis-coumarin for detection of hydrazine. Tetrahedron. 2020 Feb 14;76(7).

21. Tasior M, Kim D, Singha S, Krzeszewski M, Ahn KH, Gryko DT. π-Expanded coumarins: Synthesis, optical properties and applications. J Mater Chem C Mater. 2015 Feb 21;3(7):1421–46.

22. Tasior M, Poronik YM, Vakuliuk O, Sadowski B, Karczewski M, Gryko DT. V-shaped bis-coumarins: Synthesis and optical properties. Journal of Organic Chemistry. 2014 Sep 19;79(18):8723–32.

23. Raunio H, Pentikäinen O, Juvonen RO. Coumarin-based profluorescent and fluorescent substrates for determining xenobiotic-metabolizing enzyme activities in vitro. Int J Mol Sci. 2020 Jul 1;21(13):4708.

24. Luan C, Yang Z, Chen B. Signal Improvement Strategies for Fluorescence Detection of Biomacromolecules. J Fluoresc. 2016 May;26(3):1131-9.

25. James J Pitt. Principles and Applications of Liquid Chromatography - Mass Spectrometry in Clinical Biochemistry. Clin Biochem Rev. 2009 Feb;30(1):19-34.

26. Beccaria M, Cabooter D. Current developments in LC-MS for pharmaceutical analysis. Analyst. Royal Society of Chemistry. 2020;145:1129–57.

27. Cuyckens F. Mass spectrometry in drug metabolism and pharmacokinetics: Current trends and future perspectives. Rapid Communications in Mass Spectrometry. 2019;33(S3):90–5.

28. Zhou B, Xiao JF, Tuli L, Ressom HW. LC-MS-based metabolomics. Molecular BioSystems. Royal Society of Chemistry. 2012;8:470–81.

29. Fang ZZ, Gonzalez FJ. LC-MS-based metabolomics: An update. Arch Toxicol. 2014 Aug;88(8):1491-502.

30. Xiao JF, Zhou B, Ressom HW. Metabolite identification and quantitation in LC-MS/MS-based metabolomics. Trends Analyt Chem. 2012 Feb 1;32:1-14.

31. Kostiainen R, Kotiaho T, Kuuranne T, Auriola S. Liquid chromatography/atmospheric pressure ionization - Mass spectrometry in drug metabolism studies. J Mass Spectrom. 2003 Apr;38(4):357-72.

32. Saurina J, Sentellas S. Liquid chromatography coupled to mass spectrometry for metabolite profiling in the field of drug discovery. Expert Opin Drug Discov. 2019 May;14(5):469-483.

33. Vogeser M, Parhofer KG. Liquid chromatography tandem-mass spectrometry (LC-MS/MS) - Technique and applications in endocrinology. Exp Clin Endocrinol Diabetes. 2007 Oct;115(9):559-70.

34. Lu X, Zhao X, Bai C, Zhao C, Lu G, Xu G. LC-MS-based metabonomics analysis. J Chromatogr B Analyt Technol Biomed Life Sci. 2008 Apr 15;866(1-2):64-76.

35. Zubarev RA, Makarov A. Orbitrap mass spectrometry. Anal Chem. 2013 Jun 4;85(11):5288–96.

36. Eliuk S, Makarov A. Evolution of Orbitrap Mass Spectrometry Instrumentation. Annu Rev Anal Chem (Palo Alto Calif). 2015;8:61-80.

37. Perry RH, Cooks RG, Noll RJ. Orbitrap mass spectrometry: Instrumentation, ion motion and applications. Mass Spectrom Rev. 2008 Nov;27(6):661–99.

38. Makarov A, Scigelova M. Coupling liquid chromatography to Orbitrap mass spectrometry. J Chromatogr A. 2010 Jun 18;1217(25):3938-45.

39. de Hoffmann E, Stroobant V. Mass Spectrometry Principles and Applications. Wiley. 2007;3:502.

40. Sawada Y, Yokota Hirai M. Integrated LC-MS/MS system for plant metabolomics. Comput Struct Biotechnol J. 2013 May 23;4:e201301011.

41. Perez de Souza L, Alseekh S, Scossa F, Fernie AR. Ultra-high-performance liquid chromatography high-resolution mass spectrometry variants for metabolomics research. Nat Methods. 2021 Jul;18(7):733-746.

42. Juvonen RO, Pentikäinen O, Huuskonen J, Timonen J, Kärkkäinen O, Heikkinen A, et al. In vitro sulfonation of 7-hydroxycoumarin derivatives in liver cytosol of human and six animal species. Xenobiotica. 2020 Aug 2;50(8):885–93.

43. Zanger UM, Schwab M. Cytochrome P450 enzymes in drug metabolism: Regulation of gene expression, enzyme activities, and impact of genetic variation. Pharmacol Ther. 2013 Apr;138(1):103-41.